

# Incorporating kinematic attributes into rock glacier inventories exploiting InSAR data: preliminary results in eleven regions worldwide Incorporating InSAR kinematics into rock glacier inventories: Insights from eleven regions worldwide

5 Aldo Bertone<sup>1,2\*</sup>, Chloé Barboux<sup>2</sup>, Xavier Bodin<sup>3</sup>, Tobias Bolch<sup>4</sup>, Francesco Brardinoni<sup>1</sup>, Rafael Caduff<sup>5</sup>,  
Hanne H. Christiansen<sup>6</sup>, Margaret M. Darrow<sup>7</sup>, Reynald Delaloye<sup>2</sup>, Bernd Etzelmüller<sup>8</sup>, Ole Humlum<sup>6,8</sup>,  
Christophe Lambiel<sup>9</sup>, Karianne S. Lilleøren<sup>8</sup>, Volkmar Mair<sup>10</sup>, Gabriel Pellegrinon<sup>1</sup>, Line Rouyet<sup>11</sup>, Lucas  
Ruiz<sup>12</sup>, Tazio Strozzi<sup>5</sup>

1 Department of Biological, Geological and Environmental Sciences, University of Bologna, Bologna, 40126, Italy

10 2 Department of Geosciences, Geography, University of Fribourg, Fribourg, 1700, Switzerland

3 Laboratoire EDYTEM, CNRS/Université Savoie Mont-Blanc, Le Bourget-du-Lac, 73370, France

4 School of Geography & Sustainable Development, University of St Andrews, St Andrews, KY16 9AL, United Kingdom

5 Gamma Remote Sensing, Gümligen, 3073, Switzerland

6 Arctic Geology Department, The University Centre in Svalbard, Longyearbyen, 156 N-9171, Svalbard

15 7 Department of Civil, Geological, and Environmental Engineering, University of Alaska Fairbanks, Fairbanks, Alaska, 99775-5900, USA

8 Department of Geosciences, University of Oslo, Oslo, 0316, Norway

9 Institute of Earth Surface Dynamics, University of Lausanne, Lausanne, 1015, Switzerland

10 10 Office for Geology and Building Materials Testing, Autonomous Province of Bolzano, Bolzano, 39100, Italy

20 11 Department of Technology, NORCE Norwegian Research Centre AS, Troms, 9019, Norway

12 Argentine Institute of Nivatology, Glaciology and Environmental Sciences, CCT CONICET Mendoza, Mendoza, 5500, Argentina

Correspondence to: Aldo Bertone (aldo.bertone@unibo.it)

## Abstract.

25 The dependence of Rock glaciers ~~contain~~ are landforms related to ~~on~~ permafrost creep, which ~~and thus~~ their sensitivity are  
sensitive to climate ~~ie~~ parameters variability and change ~~makes the~~ ~~Their~~ spatial distribution of these landforms and kinematic  
behaviour can be ~~very important~~ critical for ~~managing~~ water resources and ~~geohazards~~ potential in ~~periglacial areas~~ hydrological  
and ~~climate changes~~ reasons. Inventories of Rock glaciers have been ~~produced~~ ~~inventoried~~ for decades worldwide, often  
30 without ~~an~~ assessment of their kinematics. ~~t~~The availability of remote sensing data makes ~~however~~ the inclusion of kinematic  
information potentially feasible, but ~~the absence of~~ ~~requires~~ a common methodology ~~makes it challenging~~ ~~in order~~ to create  
homogeneous inventories. In this context, the International Permafrost Association (IPA) Action Group on rock glacier  
inventories and kinematics (2018-2023), with the support of the European Space Agency (ESA) Permafrost Climate Change  
Initiative (CCI) project, is ~~promoting the~~ ~~defining~~ ~~of~~ standard guidelines for the inclusion of kinematic information within  
35 inventories. Here, we ~~test~~ ~~demonstrate~~ the feasibility of applying common rules proposed by the Action Group in eleven  
regions worldwide. Spaceborne interferometric synthetic aperture radar (InSAR) ~~Satellite interferometry~~ is used to characterize

identifiable moving areas ~~with slope movements~~ related to rock glaciers. Subsequently, these areas are used to assign a kinematic information to rock glaciers in existing or newly compiled inventories. More than 5,000 ~~slope movements~~moving areas and more than 3,600 rock glaciers are classified according to their kinematics. ~~The method and After The analyzes conducted on the method and on~~ the preliminary results ~~are analysed~~are observed. We identified some drawbacks ~~show small irregularities~~ related to the ~~detection capacity~~ intrinsic limitations of InSAR interferometry and to various applied strategies regarding the integration of non-moving rock glaciers ~~the lack of rock glaciers without detectable movements~~ in some investigated regions ~~investigated~~are observed. This is the first internationally coordinated work that incorporates effort of rock glacier inventories. We demonstrate the feasibility of applying common rules to implement kinematic attributes within rock glacier inventories at a global scale, despite the various regions and intensive manual effort. The results show the value of designing standardized inventorying procedures for periglacial geomorphology.

## 1 Introduction

Rock glaciers are creeping masses of frozen debris, ~~detectable~~ in the mountain periglacial landscape ~~by the following~~ ~~Morphologically, they are characterised by a distinctes~~ front, lateral margins, and ~~optionally often by~~ ridge-and-furrow surface topography (Barsch, 1996; Haeberli et al., 2006; Berthling, 2011; Haeberli et al., 2006). These landforms are frequently used as a proxy for permafrost occurrence in cold mountain regions (Haeberli, 1985; Boeckli et al., 2012; Schmid et al., 2015; Haeberli, 1985; Marcer et al., 2017; Schmid et al., 2015; Scotti et al., 2017), and can be important for ice (water) storage estimation (Corte, 1976; Bolch et al., 2009; Azócar and Brenning, 2010; Boeh et al., 2009; Corte, 1976; Jones et al., 2018a), geohazard management (Delaloye et al., 2013; Kummert et al., 2018), as well as climate reconstruction (Konrad et al., 1999; Kääb et al., 2007, 2021; Konrad et al., 1999).

The spatial distribution of rock glaciers is generally investigated with the support of geodatabases defined as inventories. Initiatives have risen for decades for inventorying rock glaciers in the main periglacial mountain regions of the world, such as in Asia (e.g., Gorbunov et al., 1998; Schmid et al., 2015; Wang et al., 2017; Jones et al., 2018b; Blöthe et al., 2019; Bolch et al., 2019; Gorbunov et al., 1998; Jones et al., 2018b; Reinosch et al., 2021; Schmid et al., 2015; Wang et al., 2017), North America (e.g., Liu et al., 2013; Charbonneau and Smith, 2018; Liu et al., 2013; Munroe, 2018), South America (e.g., Rangecroft et al., 2014; Falaschi et al., 2015; Barcaza et al., 2017; Falaschi et al., 2015; Rangecroft et al., 2014; Villarroel et al., 2018; Zalazar et al., 2020), New Zealand (e.g., Sattler et al., 2016; Lambiel et al., 2019; Sattler et al., 2016), European Alps (e.g., Guglielmin and Smiraglia, 1998; Delaloye et al., 2010; Cremonese et al., 2011; Krainer and Ribis, 2012; Seppi et al., 2012; Scotti et al., 2013; Barboux et al., 2015; Colucci et al., 2016; Cremonese et al., 2011; Delaloye et al., 2010; Guglielmin and Smiraglia, 1998; Krainer and Ribis, 2012; Scotti et al., 2013; Seppi et al., 2012; Wagner et al., 2020), Carpathians (e.g., Necsoiu et al., 2016) and Scandinavia (e.g., Lilleøren and Etzelmüller, 2011; Lilleøren et al., 2013).

In 2018, Jones et al. (2018) provided an overview of available rock glacier inventories ~~on~~ at a global scale, counting more than 130 inventories worldwide, of which over 90 % were produced after the year 2000s. The authors merged all these available

inventories to create a global inventory, in order to provide a first-order approximation of volumetric ice content contained within rock glaciers. Their analysis highlighted several limitations on the current inventories, namely the absence of an accessible open-access database, the heterogeneities/variabilities of the existing inventories (due to unequal availability of data sources and on variable local geomorphological skills and institutional support), and the subjectivity in the manual identification of rock glaciers, as also observed by Brardinoni et al. (2019). The authors noted that the main limitation is the absence of a common methodology to provide standardized inventories, making it challenging to create a homogeneous global inventory. Nowadays, the international cooperation of the scientific community represents the key element to solve these open questions.

The International Permafrost Association (IPA) Action Group on Rock Glacier Inventories and Kinematics, launched in 2018 (Delaloye et al., 2018), intends to sustain the establishment of widely accepted baseline concepts and standard guidelines for inventorying rock glaciers in mountain permafrost regions (IPA Action Group RGIK – baseline concepts, 2022). For the IPA community, a crucial element to include in standardized rock glacier inventories is the kinematic information. Indirect kinematic information – frequently imprecise because related to the operator's interpretations – are often derived from visual observation of morphological (e.g., front slope angle) and vegetation-related indicators (Barsch, 1992; Brardinoni et al., 2019). More precise and accurate approaches based on remote sensing data (e.g., satellite interferometry with Sentinel-1 images; Yague-Martinez et al., 2016) were developed ~~in literature~~ to characterize the rock glacier kinematics at a large-scale (Neesoij et al., 2016; Wang et al., 2017; Villarroel et al., 2018; Strozzi et al., 2020; Brencher et al., 2021; Neesoij et al., 2016; Strozzi et al., 2020; Villarroel et al., 2018; Wang et al., 2017). These latter approaches are nevertheless based on different criteria and still lack standardized outputs (Jones et al., 2018a; Brardinoni et al., 2019; Jones et al., 2018a), essential to integrate kinematic information in standardized rock glacier inventories. In this context, ~~a part of the European Space Agency (ESA) Permafrost Climate Change Initiative (Permafrost\_CCI) project so-called CCN2~~ (<https://climate.esa.int/en/projects/permafrost/>; last access: 10 October 2021) – following the baseline concepts proposed by the IPA Action Group (IPA Action Group RGIK – baseline concepts, 2022; RGIK - kinematic, 2022) – developed specific guidelines (IPA Action Group RGIK - kinematic approach, 2020) to systematically integrate kinematic information within rock glacier inventories, exploiting spaceborne ~~Interferometric Synthetic Aperture Radar (InSAR) data. The guidelines define common rules, intended at reducing subjectivity, which is a potential source of uncertainty and variability. To summarize the workflow, moving areas identified as slope with actual movements are first delineated and characterized in terms of velocity class based on interferometric data.~~ The inventoried ~~slope movements~~ ~~moving areas~~ are then used to assign kinematic information to rock glaciers. Existing rock glacier inventories or newly compiled inventories are exploited to circumscribe the identification of ~~moving areas~~ ~~slope movements~~.

Here ~~In this work, our main aim is to~~ ~~we~~ present the ~~developed~~ guidelines ~~developed within the -ESA Permafrost –CCI project and in collaboration with the IPA Action Group (IPA Action Group RGIK~~ - kinematic approach, 2020). ~~Our main aim is to and test~~ ~~explore and demonstrate~~ the feasibility of an international ~~joint effort~~ ~~cooperation~~ to include kinematic information in rock glacier inventories (RoGI). ~~To achieve this goal, we applying~~ the ~~aforementioned~~ guidelines in eleven ~~different~~

105 ~~periglacial~~ regions of the world. ~~The guidelines define common rules, intended at reducing subjectivity, which is a potential source of uncertainty and variability. To summarize the workflow, areas identified as slope movements are first delineated and characterized in terms of velocity class based on interferometric data. The inventoried slope movements are then used to assign kinematic information to rock glaciers. Existing rock glacier inventories or newly compiled inventories are exploited to circumscript the identification of slope movements.~~

110 ~~Most existing inventories do n't not include kinematic information (Jones et al., 2018a), and Hhere we are the first to apply the guidelines in eleven different periglacial regions of the world and consistently derive semi-quantitative standardized kinematic information on rock glaciers in over as many regions all around the globe as possible. This paper includes the description of the~~ ~~As this paper is the result of a very large cooperative work building upon recently published guidelines, it cannot present perfect results and definitive statements; therefore, it doesn't focus on the interpretation and comparison of investigated RoGIs. Here wWe guidelines, and present a collection of products result obtained in the investigated regions, including as well as also analyzes analyses, observations and general considerations based on deduced aimed at studying irregularities and differences observed from the observations results obtained.~~ A product validation is also conducted with 115 independent measurements ~~in~~ some specific cases. ~~As this paper is the result of a very large cooperative work and builds in upon recently published guidelines, it does cannot present perfect definitive results and conclusions definitive statements; On this premise, aAt this stage we are not concerned with therefore, it doesn't focus on the exhaustive interpretation and critical comparison of the eleven investigated RoGIs. Finally We focus here on Rather, we discussing the advantages and limitations and potentials of the proposed standardized approach guidelines and their potential to support the integration of kinematic~~ 120 information ~~within~~ inventories at a global scale.

## 2 Study areas and dataset

125 We investigate eleven periglacial regions with various environmental parameters distributed around the world (Fig. 1, Table 1), covering eight major mountain ranges over five continents. Their spatial extent ranges from 250 to 7200 km<sup>2</sup> (Table 1), with an approximate median of 1600 km<sup>2</sup>. ~~All The~~ study areas ~~have are in~~ permafrost conditions, but in some places only in the higher parts of the landscape.

130 Three study sites are located in the European Alps: Western Swiss Alps (Switzerland), Southern Vinschgau/ Venosta Valley (Italy), Vanoise Massif (France); five study sites are located in the sub-Arctic to high Arctic regions: Troms and Finnmark (Northern Norway), Nordenskiöld Land (Svalbard), Disko Island (Greenland), Brooks Range (Alaska, USA); one site ~~is~~ in Central Asia: Northern Tien Shan (Kazakhstan); one site ~~is~~ in South America: Central Andes (Argentina); one site ~~is~~ in Oceania: Central Southern Alps (New Zealand).

In Nordenskiöld Land (Svalbard), an entirely new rock glacier inventory is generated. For the remaining ten regions, existing inventories or partial inventories ~~we are~~ available. Detailed information on the geographical parameters of these investigated

regions and references to the available rock glacier inventories are presented in Table 1. Additional information for each region is included in Supplementary material A “Description of study areas”.

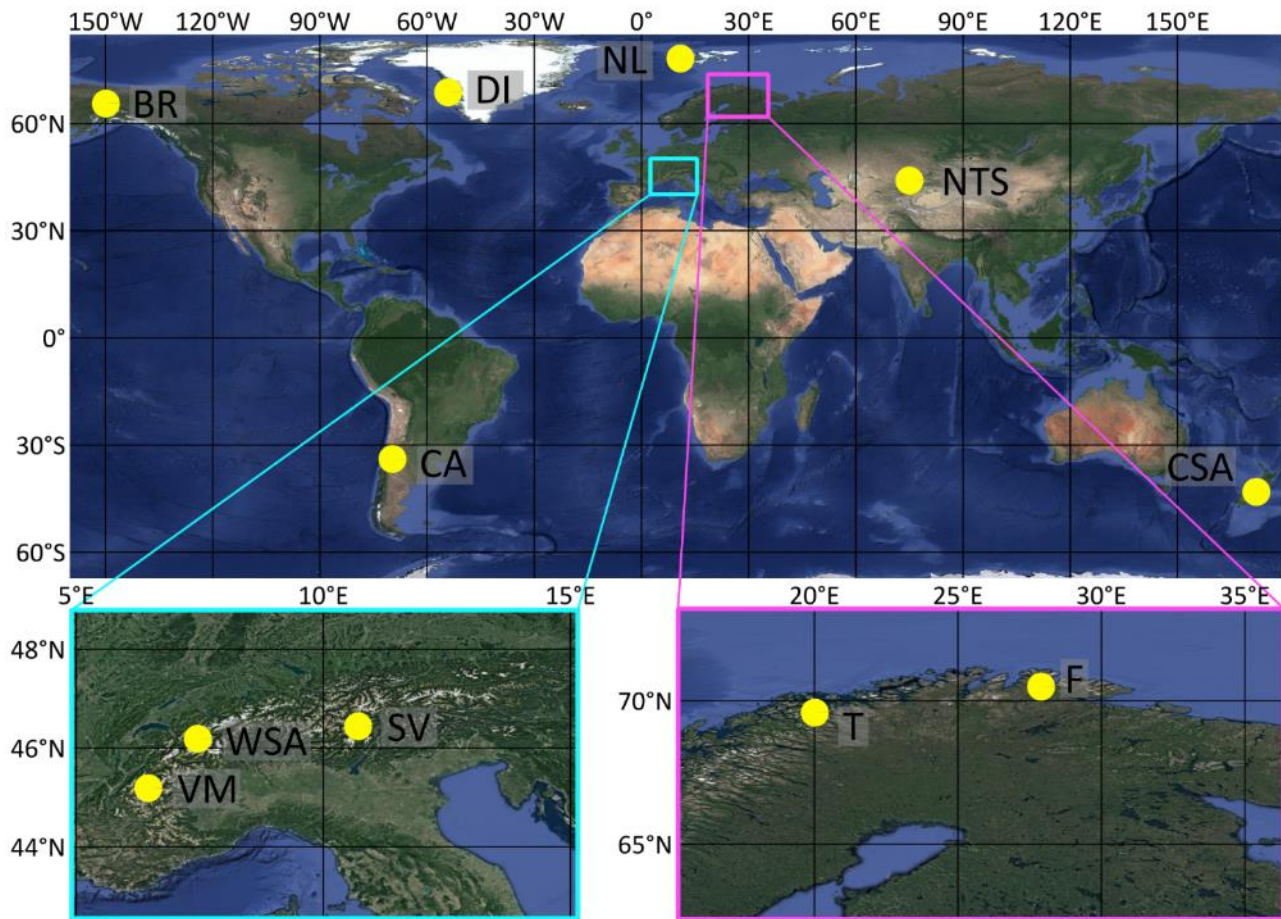
135 Synthetic aperture radar (SAR) data from the Sentinel-1 (S1) and ALOS-2 satellites used in the present work (Table 1) are collected in both SAR geometries (i.e., ascending and descending) to ensure the best line-of-sight (LOS) orientation ([Liu et al., 2013](#); [Barboux et al., 2014](#); [Liu et al., 2013](#)). As snow cover is a severe limitation for InSAR (Klees and Massonnet, 1998), only snow-free periods are considered ([from July to September and from January to March for Northern and Southern Hemisphere, respectively](#)). [Any residual snow periods are detected by identifying extended interferometric decorrelation and by exploiting the interferometric evidence on InSAR data evidence \(e.g., extended interferometric decorrelation, Touzi et al., 1999\)](#) on. Sentinel-1 images are acquired in Interferometric Wide swath mode with a 250 km swath at 5 m (range) by 20 m (azimuth) spatial resolution. ALOS-2 images are collected in Fine mode with a swath width of 70 km and spatial resolution of about 10 m (both range and azimuth). The information on the satellite data used and the time intervals considered for the investigated regions are presented in Table 1.

145 Depending on availability in each region, additional data such as aerial orthoimages, digital terrain models (DTMs) and DTM-derived products (e.g., hillshade) are included. The complete list of data used for each investigated region is included in Supplementary material A “Description of study areas”. Additional kinematic measurements from differential global navigation satellite system (DGNSS) available for 17 rock glaciers in the Western Swiss Alps ([Delaloye and Staub, 2016](#); [Kummert and Delaloye, 2018](#); [Noetzli et al., PERMOS, 2019](#); [Strozzi et al., 2020](#)), Vanoise ([Marcer et al., 2020](#)), Nordenskiöld 150 Land ([Matsuoka et al., 2019](#)), Central Andes ([Blöthe et al., 2021](#)), Central Southern Alps regions, and for four frozen debris lobes (FDLs) in the Brooks Range ([Darrow et al., 2016](#)) are used for qualitative validations. For the purposes of this study, measurements of FDLs are not differentiated from rock glaciers for the Brooks Range study area. Feature tracking measurements on optical aerial photographs are also [conducted available](#) for nine rock glaciers in the Troms ([Eriksen et al., 2018](#)), Nordenskiöld Land, and Northern Tien Shan ([Bolch and Strel, 2018](#); [Kääb et al., 2021](#)) regions.

155

**Table 1. Descriptions of geographic settings, rock glacier inventory (RoGI) references and InSAR data used for each investigated region.**

Western Swiss Alps, Switzerland 46°N 7.5°E	Extent [km <sup>2</sup> ] Altitude range [m a.s.l.] Annual Precipitation range [mm] Reference RoGI InSAR data used (time intervals)	1100 1250 – 4600 1100-1700 (Barboux et al., 2015) S1 (2018-2019)
Southern Venosta, Italy 46.5°N 10.9°E	Extent [km <sup>2</sup> ] Altitude range [m a.s.l.] Annual Precipitation range [mm] Reference RoGI InSAR data used (time intervals)	970 500-3900 600-1200 (Mair et al., 2008) S1 (2018-2019)
Vanoise, France 45.4°N 6.9°E	Extent [km <sup>2</sup> ] Altitude range [m a.s.l.] Annual Precipitation range [mm] Reference RoGI InSAR data used (time intervals)	2000 700-3900 1000-1600 (Marcer et al., 2017) S1 (2016-2019)
Troms, Norway 69.5°N 20°E	Extent [km <sup>2</sup> ] Altitude range [m a.s.l.] Annual Precipitation range [mm] Reference RoGI InSAR data used (time intervals)	4400 0-1800 700-1300 (Lilleøren and Etzelmüller, 2011) S1 (2015-2019)
Finnmark, Norway 70.7°N 27.9°E	Extent [km <sup>2</sup> ] Altitude range [m a.s.l.] Annual Precipitation range [mm] Reference RoGI InSAR data used (time intervals)	2600 0-700 500-900 (Lilleøren and Etzelmüller, 2011) S1 (2015-2020)
Nordenskiöld Land, Svalbard 78°N 15.5°E	Extent [km <sup>2</sup> ] Altitude range [m a.s.l.] Annual Precipitation range [mm] Reference RoGI InSAR data used (time intervals)	4100 0-1200 400-1000 New S1 (2015-2020)
Disko Island, Greenland 70°N 53°W	Extent [km <sup>2</sup> ] Altitude range [m a.s.l.] Annual Precipitation range [mm] Reference RoGI InSAR data used (time intervals)	7200 900-1900 300-500 (Humlum, 1982) S1 (2015-2019), ALOS-2 (2015-2017)
Brooks Range, Alaska 68°N 150°W	Extent [km <sup>2</sup> ] Altitude range [m a.s.l.] Annual Precipitation range [mm] Reference RoGI InSAR data used (time intervals)	1250 900-2400 200-400 (Ellis and Calkin, 1979) S1 (2016-2019), ALOS-2 (2015-2016)
Northern Tien Shan, Kazakhstan 43°N 77°W	Extent [km <sup>2</sup> ] Altitude range [m a.s.l.] Annual Precipitation range [mm] Reference RoGI InSAR data used (time intervals)	250 1000-5000 800-1300 (Bolch and Gorbunov, 2014) S1 (2018-2019), ALOS-2 (2015-2016)
Central Andes, Argentina 33°S 69.6°W	Extent [km <sup>2</sup> ] Altitude range [m a.s.l.] Annual Precipitation range [mm] Reference RoGI InSAR data used (time intervals)	2900 2000-6000 400-500 (Zalazar et al., 2020) S1 (2018-2020), ALOS-2 (2016-2019)
Central Southern Alps, New Zealand 43°S 170°E	Extent [km <sup>2</sup> ] Altitude range [m a.s.l.] Annual Precipitation range [mm] Reference RoGI InSAR data used (time intervals)	4800 500-3700 1000-14000 (Sattler et al., 2016) S1 (2018-2019)



160 **Figure 1.** Location of the eleven investigated regions (yellow dots): Nordenskiöld Land (NL), Disko Island (DI), Brooks Range (BR),  
 Northern Tien Shan (NTS), Central Andes (CA) and Central Southern Alps (CSA). Western Swiss Alps (WSA), Southern Venosta (SV), Vanoise Massif (VM), Troms (T) and Finnmark (F) are visible in two enlarged panels. Orthoimages from © Google Earth 2019.

### 3 Methods

#### 3.1 Workflow and input data

165 The technical aspects related to rock glaciers and presented below are contained in the [baseline concepts](#) documents of the IPA Action Group ([IPA Action Group RGIK](#) - baseline concepts, 2020; [RGIK - kinematic, 2022](#)). These [documents](#) [baseline concepts](#) are constantly discussed and updated by the scientific community, and are therefore susceptible to changes, evolutions and improvements. This work [is in accordance with](#) [refers to](#) the versions [of the baseline concepts](#) produced in [March](#) and [May](#) 2020. A rock glacier inventory consists of a geodatabase, containing the rock glaciers' locations as points and additional information such as activity rates and geomorphological parameters. Optional information, such as the geomorphological delineations with polygons, can be included. [Hereafter, the term rock glacier refers to the](#) A rock glacier – and precisely a rock

175 ~~glacier~~ unit (RoG) — is defined as a single lobate structure that can be unambiguously discerned according to morphologic evidence such as frontal slope, lateral margins, and ridge-and-furrow topography ([RGIK - baseline concepts, 2022](#)). The spatial connection from other (adjacent or overlapping) ~~rock~~ ~~glacier~~ units can be determined by distinguishing different generations of landforms (e.g., overlapping lobes), different connections to the upslope unit, or specific activity rates. A rock glacier “unit” is differentiated from a rock glacier “system” (i.e., a landform identified as a rock glacier), which is composed of either one single or multiple rock glacier “units” that are spatially connected either in a toposequence or in coalescence. Because of practical and technical limitations, the minimum size of a considered rock glacier unit is [about](#) 0.01 km<sup>2</sup>.

180 The systematic procedure contained in the guidelines ([IPA Action Group RGIK - kinematic approach, 2020](#)) follows the baseline concepts ([IPA Action Group RGIK - baseline concepts, 2020; RGIK - kinematic, 2022](#)) and consists of three phases described below and illustrated in Fig. 2. The aim of this procedure is to implement the kinematic information in the inventories, especially to the rock glaciers affected by movement, to reduce the subjectivity of operators' interpretations and thus have a more accurate and standardized classification.

185 The first phase consists of the identification of rock glaciers. For this purpose, existing rock glacier inventories or other forms of information such as from the literature are used. When inventories are not available over the investigated region (e.g., Nordenskiöld Land), the landform identification is performed following the baseline concepts proposed by the IPA Action Group ([IPA Action Group RGIK - baseline concepts, 2020](#)); systematic visual analysis of the landscape with satellite or airborne optical images (orthoimages and DTM-derived products), field visiting, or supervised/unsupervised methods that allow a systematic identification of rock glaciers can be used (Marcer, 2020; Robson et al., 2020). Within this work, the 190 identified rock glaciers are distinguished using manually positioned dots on each landform, able to discriminate each rock glacier clearly without ambiguity (e.g., in the center of the lobe of the ~~rock~~ ~~glacier~~ unit [RoG](#)). This initial phase is very important, because the greater the completeness of the rock glaciers identified, the greater the completeness of the products obtained in the following two phases.

195 The second phase ~~consists~~consists of identifying, outlining, and assigning velocity classes to moving areas (MA) – i.e., areas identified as having slope movement with InSAR data – related to the previously identified rock glaciers. Moving areas are included within inventories [using](#) [through](#) [polygons](#). This phase is conducted in parallel with the rock glacier identification, because additional landforms potentially missed can be identified when characterized by moving areas through an iterative process between the identifications of moving areas and rock glaciers.

200 The third phase ~~consists~~consists of assigning kinematic attributes to rock glaciers by exploiting the velocity classes and extents of the moving areas that cover the rock glaciers. This information is then implemented within the inventory. [Thus, a kinematic attribute represents the overall movement rate of a rock glacier, while the moving areas document the detailed velocity distribution](#) [provide the detailed kinematics within the rock glacier](#).

205 In this work, further phases of semi-quantitative assessments are conducted on specific rock glaciers to verify the correctly assigned kinematic categories, comparing the moving area velocity classes and the rock glacier kinematic attributes with independent measurements acquired during the same time frame. An additional effort adopted to further reduce the

subjectivity, misclassifications, errors and increase the overall reliability of the products consists of multiple phases of correction and adjustment conducted by a second operator. ~~In detail, the results produced by the first operator are checked by a second operator, thus exploiting the knowledge of two different operators.~~ In order to optimize the work, operators with both InSARinterferometrie and geomorphological- backgrounds are involved, and study areas already known by the operators are considered to make the best use of the operators' knowledge.

Below in Sect. 3.2 we introduce the basic principles of InSAR. Subsequently in Sect. 3.3 ~~we describe the details of the we present the standards of moving areas and the InSARinterferometric~~ methods used to produce the moving area inventories. The procedure to assign a kinematic attribute to a rock glacier is described in Sect. 3.4. More details are further described in the practical guidelines (IPA Action Group RGIK - kinematic approach, 2020) and in Table SB1 and SB2.

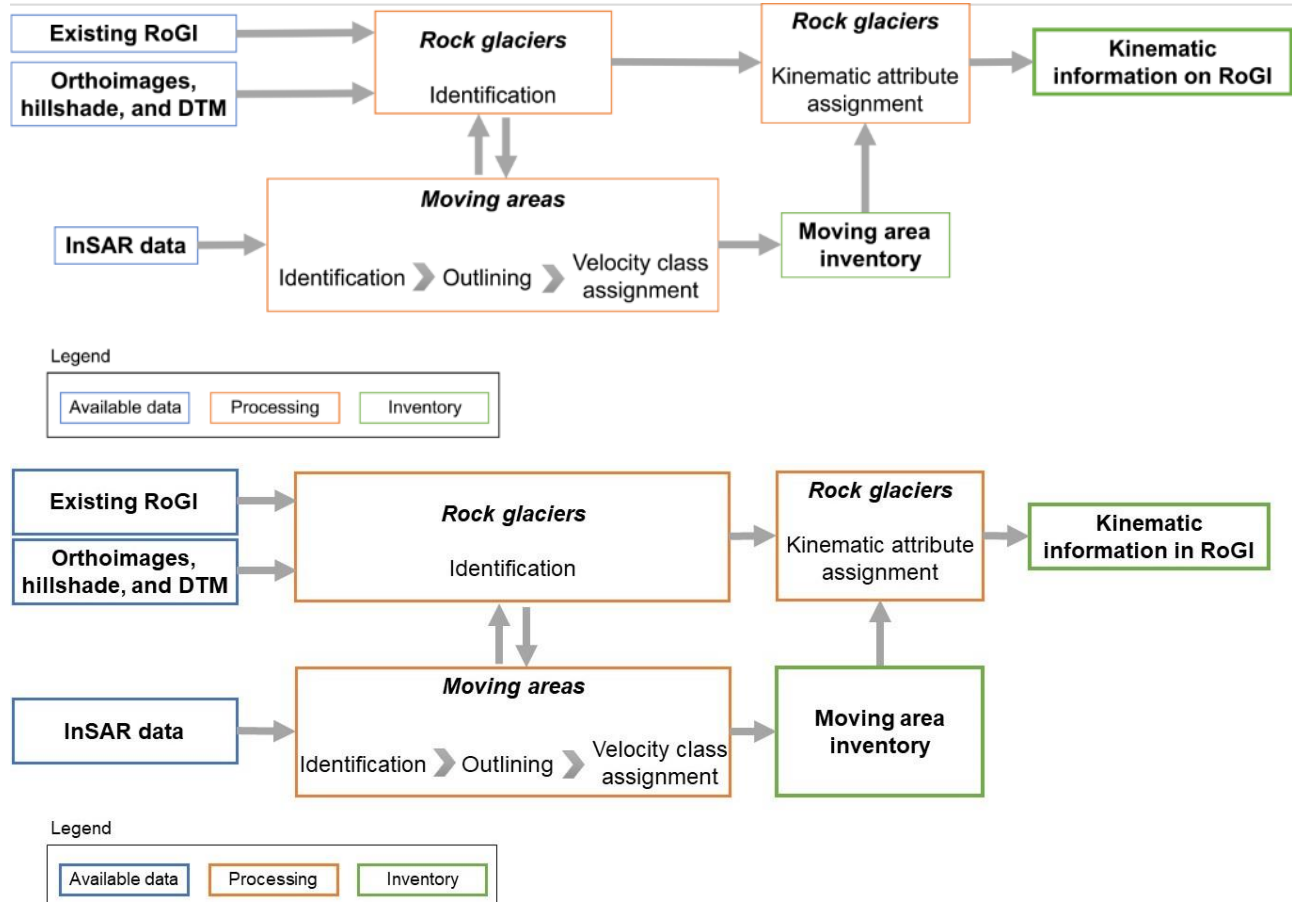


**Figure 2.** Conceptual diagram of the standardized method for producing a moving area inventory and a rock glacier inventory (RoGI) ~~that includes kinematic information by including kinematics~~. The analysis is performed in a GIS environment.

### 3.2 Basic principles of Interferometric Synthetic Aperture Radar (InSAR)

220 InSAR is a powerful and consolidated techniques to detect and map ground movement at the regional scale (Klees and Massonnet, 1998; Massonnet and Feigl, 1998). Systematic acquisitions and wide spatial coverage of the new generation of satellites such as Sentinel-1 make InSAR the most suitable tool for the global mapping objectives of this work (Yague-Martinez et al., 2016).

225 The interferometricInSAR processing consists of computing the interferometric phase differences (i.e., the interferograms) fromby combining pairs of images with different time intervals (from a few days up to annual) (Massonnet and Souyris, 2008; Yague-Martinez et al., 2016). After geometric, topographic, and atmospheric corrections, interferograms provide quantitative measurements of the superficial movements (Klees and Massonnet, 1998; Yague-Martinez et al., 2016).

230 Despite the potential of InSAR, some limitations apply. First, InSAR provides the observation of the 3D surface deformation component projected along the radar look direction (i.e., the line of sight, LOS), and the measurement is not sensitive to displacements orienteddirected perpendicular to the LOS orientation (Liu et al., 2013; Barboux et al., 2014; Liu et al., 2013; Strozzi et al., 2020). Therefore, displacements towards north or south are more affected by geometric distortions and the magnitude of the displacements might be largely underestimated (Klees and Massonnet, 1998; Liu et al., 2013). Second, steep terrain is masked by geometric distortions known as layover and shadow in mountainous areas (Klees and Massonnet, 1998; Barboux et al., 2014; Klees and Massonnet, 1998). To reduce the above limitations, both ascending and descending geometries are used in this work, allowing the selection of the best geometry according to the orientation of each rock glacier (Barboux et al., 2014; Strozzi et al., 2020). Third, the rate of terrain movement that can be detected depends on the time interval of the interferogram, the spatial resolution, and the wavelength of the satellite (Massonnet and Feigl, 1998; Barboux et al., 2014; Villarroel et al., 2018; Massonnet and Feigl, 1998; Strozzi et al., 2020; Villarroel et al., 2018). Lastly, artefacts due to uncompensated atmospheric delays (Yu et al., 2018) and decorrelation or phase bias due to changes in physical properties of the surface (e.g., vegetation, snow, soil moisture; Klees and Massonnet, 1998; Zwieback et al., 2016) can mask the displacement measurements. To reduce these limitations, it is important to rely on a slack of several interferograms from different time periods.

### 3.3 Moving area inventory with InSAR

245 A moving area is defined in the guidelines as an area at the surface of a rock glacier in which the observed flow field (direction and velocity) is uniform (spatially consistent and homogenous). The moving area represents the movement rate of the rock glacier or part of it, detected along the one-dimensional LOS. Each moving area is related to (i) a specific “observation time window” (e.g., summer or annual) during which the movement is measured and to (ii) a specific “temporal frame” (year(s)) during which the periodic measurements are repeated and aggregated. The minimal observation time window is one month during snow-free periods, detected within a temporal frame of at least two years. These time intervals are intended to average 250 possible short, seasonal and multi-annual variations in the dynamics of rock glaciers (Wirz et al., 2016; Kellerer-Pirklbauer et

al., 2018; [Wirz et al., 2016](#)) that can distort the measurements. Observation time windows and temporal frames are documented in the produced moving area inventories.

Moving areas are identified and outlined ~~with by means of~~ polygons, when the signal of movement is detectable ~~on for at least 20-30 pixels of~~ InSAR data. A moving area does not necessarily fit the geomorphological outline of the rock glacier (Fig. 3).<sup>255</sup> For instance, a moving area can override the geomorphological limits of a rock glacier, several polygons of moving areas can be related to the same landform, and a slower moving area that incorporates one or more faster areas can exist (Fig. 3).

Standardized velocity classes are assigned to each moving area. ~~They and~~ are ~~intended meant to~~ (i) ~~to~~ facilitate the subsequent assignment of kinematic attributes to the rock glaciers, and (ii) ~~to~~ reduce ~~the error and~~ the ~~greater~~ degree of operator's subjectivity in assigning a specific velocity. ~~A small number of defined classes reduces the variability in choosing one class over another, despite generating a loss of information (i.e., precise velocities) and creating biased information when the velocities are close to the class boundaries. As the guidelines are intended to produce obtain as standardized results as possible, six main velocity classes are chosen to balance the above rationale. According to Following~~ recent studies (e.g., Barboux et al., 2014), the velocity classes, listed in order of increasing velocity, include: ~~the standardized velocity classes defined in the guidelines are respectively “Undefined” (velocity cannot be assessed reliably), “< 1 cm/yr,” “1-3 cm/yr,” “3-10 cm/yr,” “10-30 cm/yr,” “30-100 cm/yr,” and “> 100 cm/yr.” Two further additional classes are defined include: “Undefined” when velocity cannot be reliably assessed reliably and “Other” when (if) a more specific accurate velocity can be expressed assigned. These velocity classes represent reflect the spatio temporal mean movement rate, but neither a single intra-annual variation nor an extreme value. The boundaries between the classes are selected taking into account take into account the investigative capabilities of the InSAR, as interferograms with shorter time intervals allow for detection of high velocities fast movements, while interferograms with longer time intervals detect slower velocities movements. For this reason, the velocity classes are related to the time intervals at which movements are detected by a coherent signal. (For example, following Barboux et al., 2014, a coherent signal visible on annual Sentinel-1 interferograms of Sentinel 1 allows for documenting to detect velocities ranging from 0.2 cm/yr to 3 cm/yr). Moreover, the InSAR signals are frequently affected by large spatial and temporal variability (e.g., Figure 3c-3e). In order to reduce possible errors, the assigned velocity classes represent the mean movement rate in time (i.e., within the minimum observation time window and temporal frame defined above) and in space (i.e., within the outlines), and not a single intra-annual episode variation nor an extreme value. In this work, the moving areas with large variability of InSAR signal velocity are annotated.~~ For this reason, the velocity classes are related to the time intervals at which movements are detected by a coherent signal. (For example, following Barboux et al., 2014, a coherent signal visible on annual Sentinel-1 interferograms of Sentinel 1 allows for documenting to detect velocities ranging from 0.2 cm/yr to 3 cm/yr). Moreover, the InSAR signals are frequently affected by large spatial and temporal variability (e.g., Figure 3c-3e). In order to reduce possible errors, the assigned velocity classes represent the mean movement rate in time (i.e., within the minimum observation time window and temporal frame defined above) and in space (i.e., within the outlines), and not a single intra-annual episode variation nor an extreme value. In this work, the moving areas with large variability of InSAR signal velocity are annotated.

The production of moving area inventories can be accomplished following several approaches, such as manual interpretations of InSAR data (e.g., [Liu et al., 2013](#); Barboux et al., 2014, 2015; [Liu et al., 2013](#); Necsoiu et al., 2016; Villarroel et al., 2018), or supervised/unsupervised methods based on SAR images (e.g., Barboux et al., 2015; Rouyet et al., 2021). Below we describe the manual and semi-automated methods used in this work. ~~Clearly, the two methods are different and rely on different criteria. However, the relevant moving areas obtained share the same definition and the same velocity classes as defined above. In this paper, we do not aim The aim is not to compare the two methods. Rather, We we but to exploit the moving areas obtained~~

285 ~~with the different manual and semi-automated methods (i.e., manual and semi-automated) to similarly assign standardized kinematic attributes to rock glaciers, present and analyze the results obtained by establishing the standards described above.~~

With the manual approach we mainly considered wrapped differential interferograms, which can be computed using time intervals from a few days to a few years. Manual analyses of geospatial data, although time-consuming, is a common approach in geomorphology and has the advantage of allowing interpretation of decorrelated regions (Barboux et al., 2014), which would be excluded in phase unwrapping. In addition, errors in phase unwrapping – which are inevitable in rough terrain with

290 significant motion and not easily identified by the non-InSAR specialist - can bias the interpretation of fast-moving objects (Barboux et al., 2015). Nevertheless, weighted averaging (stacking; Sandwell and Price, 1998) of unwrapped 6/12 days

Sentinel-1 interferograms are also computed to facilitate the interpretation of single-wrapped interferograms. Moving areas are identified by looking at the textural image features from interferograms, according to three typical InSAR signal patterns: (1) no change defined by a plain pattern, (2) smooth change characterized by a (partial) fringe pattern, and (3) a decorrelated

295 signal expressed by a noisy pattern (Fig. 3c). The combined visualization of a large set of interferograms allows a user to draw fast moving area outlines from interferograms with shorter time intervals (e.g., 6 days for Sentinel-1) and shorter wavelengths.

300 ~~By increasing the time intervals, the drawn outlines are refined, and additional outlines (with lower velocities) are identified and drawn (Fig. 3d and 3e). As the manual method is based on a set of wrapped interferograms, focusing on single pixels risks to over-represent small and striking patterns. To avoid unrepresentative patterns, moving areas are outlined when the signal of movement is detectable for at least 20 to -30 pixels of InSAR data.~~

305 The velocity classes are assigned by counting the number of fringe cycle(s) from a point assumed as stable (outside the moving area) to the detected moving area. The number of fringe cycle(s) is counted exploiting the change of color in the resulting interferograms, following Fig. 3f. A complete fringe is equivalent to a change of half a wavelength in the LOS direction between two SAR images acquired at different times. The displacement obtained by knowing the wavelength of the satellite and the number of fringe cycle(s) is converted to velocity

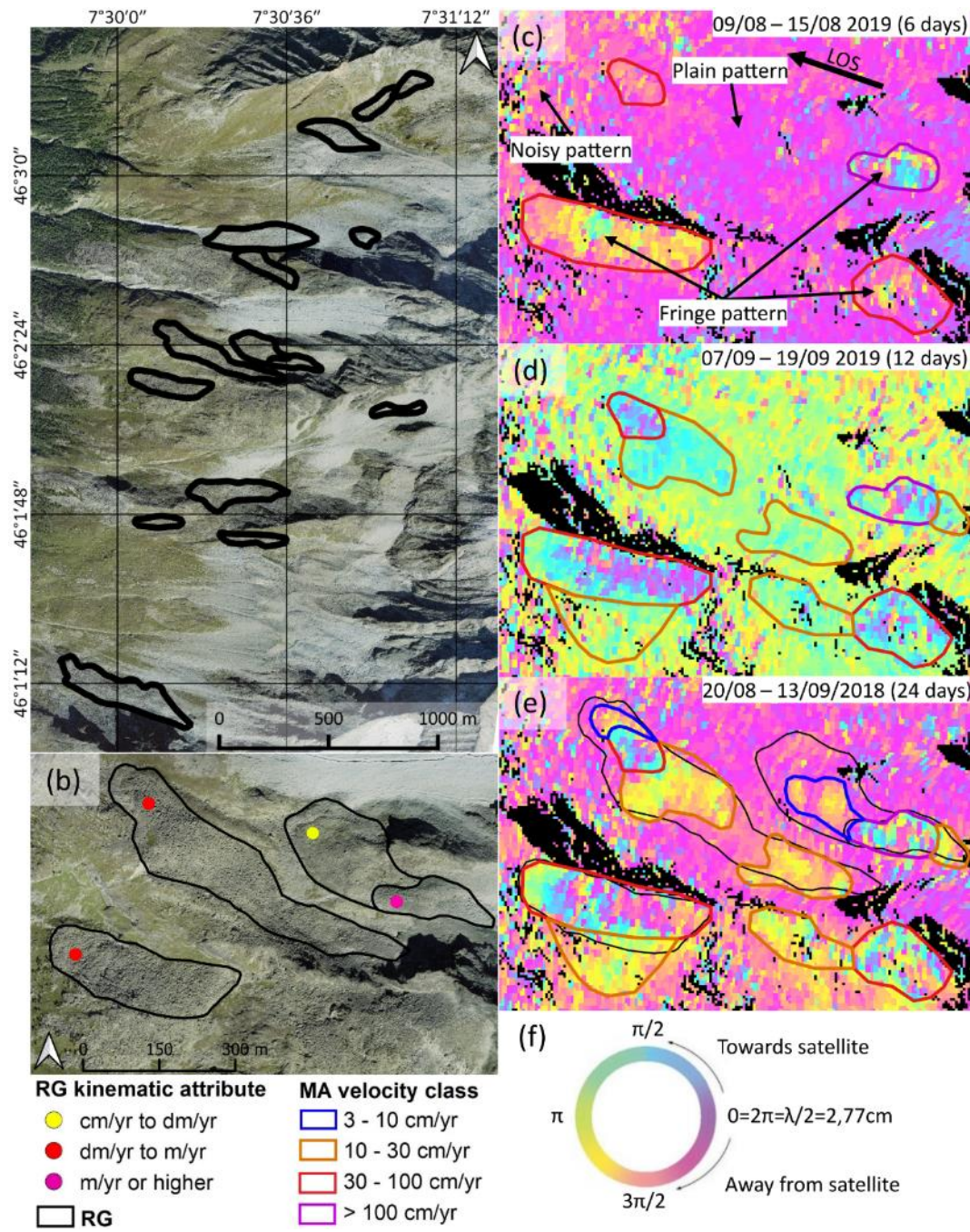
310 by dividing by the time interval of the interferogram. Detailed examples are included in Figure S1 of Supplementary material.

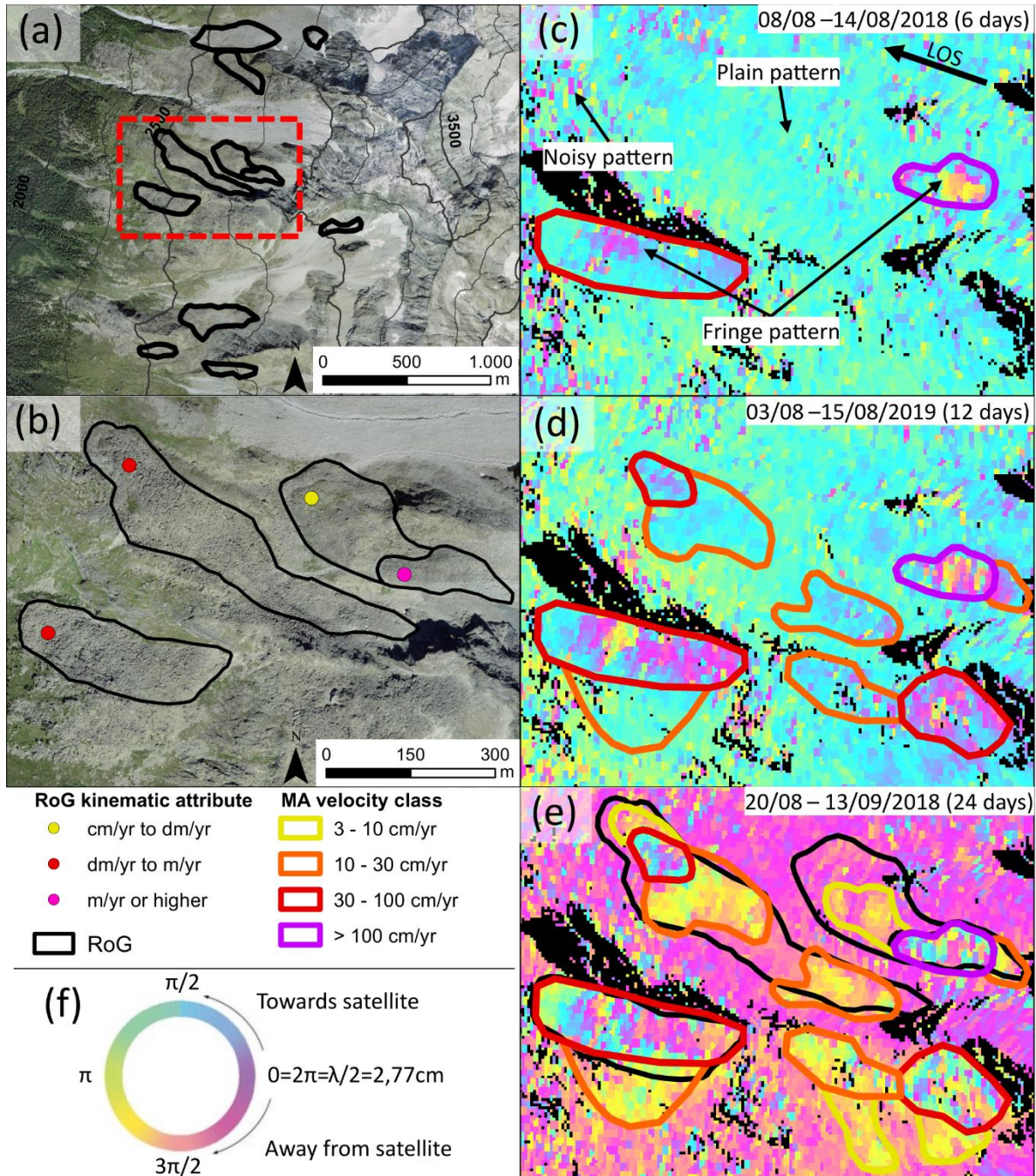
For the Norway and Svalbard study regions, a semi-automated multiple temporal baseline InSAR stacking procedure is applied (Rouyet et al., 2021). The procedure aims to combine the strengths of the single interferogram analysis and multi-temporal InSAR techniques by ~~stacking-averaging~~ unwrapped interferograms with five complementary ranges of temporal intervals (336–396, 54–150, 18–48<sup>9</sup>, 6–12 and 6 days) and complementing velocity information with mapping decorrelated signals

315 associated with fast movement. The approach ~~aims~~ to semi-automate the analysis to include a large number of interferograms (tens to hundreds for each stack) from both SAR geometries, and to combine complementary datasets with different detection capabilities, while avoiding large unwrapping errors for fast-moving landforms (Rouyet et al., 2021). The outputs of this processing are mean velocity maps with a resolution of 40 meters, on which moving areas are delineated. In particular, the velocity classes are then assigned to each pixel and all pixels are merged exploiting the entire set of pixels, i.e.,

320 ~~into a composite merged raster map over the whole area. Since each pixel is the summary of the entire multi-annual set of interferograms provides a continuous coverage over time and therefore also each single pixel is considered to be a reliable~~

representative signal of averaged movement. Compared to the manual approach, the interpretation effort is therefore reduced, but several time-consuming calibration tests are required.





320

Figure 3. Example of an RoGI in the Arolla region (location: 46°2'24"N 7°30'36"E, 2750 m a.s.l.), Swiss Alps (a); RoGI outlines of RoG are in black, and the location of an investigated area (a) is in red. (c – e) Sentinel-1 interferograms from the descending orbit, including examples of InSAR signal patterns; layover and shadow areas are masked out (black). Four Two MA signals are detected on the 6-days interferogram (c). Using 12- and 24-days, additional MA signals are visible (d and e). This is an example where the MAs outlines do not fully match the geomorphological outline of the RoGs. A fringe pattern MA (SE-border) not related to RoG is visible and mapped. Based on MAs, the kinematic attributes are assigned to RoGs (b). Fringe cycle related to the change of color (f); a complete fringe cycle is equivalent to a change of half a wavelength (2.77 cm for Sentinel-1) in the LOS direction.

### 3.4 Kinematics in the rock glacier inventory

A kinematic attribute is defined in the guidelines as semi-quantitative (order of magnitude) information, representative of the movement rate of an inventoried rock glacier. It is assigned only when spatially representative of the rock glacier, i.e., when the rock glacier is documented by consistent kinematic information on a significant part (i.e., at least half) of its surface. Kinematic attributes refer to a multi-annual validity time frame of at least two years (same temporal frame as for the moving area inventory) to minimize the potentially large inter-annual variations of rock glacier movement rate (Wirz et al., 2016; Kellerer-Pirklbauer et al., 2018; Wirz et al., 2016).

One kinematic attribute is assigned to each rock glacier unit, based on the characteristics (i.e., the extent, velocity class and time interval of observations) of the moving area(s) identified within each at the surface of the rock glacier itself are used to assign the kinematic attributes (Table 2; IPA Action Group RGIK - kinematic approach, 2020; RGIK - kinematic, 2022). Only one kinematic category is assigned per rock glacier unit; however, When a rock glacier is covered by hosts multiple dominant moving area moving areas (Sect. 3.3) a set of specific decision rules is followed rarely covers a rock glacier as a whole. When

In case of two equally dominant moving areas, characterized by contiguous but directly adjoining velocity classes, categories occur on a rock glacier, the category the velocity class of the most representative moving area (e.g., the one closest to the front, according to Barsch, 1996) is favored for the attribution of kinematic attribute to the rock glacier. In the case of a higher number more extensive spread of equally dominant velocity classes categories on the same rock glacier, the median category class is retained. Heterogeneities of moving areas inside a rock glacier can also indicate the need to refine/redefine the delineation of the initial geomorphological units, following an iterative process between geomorphology and kinematics.

A manual transfer from velocity classes of moving areas to kinematic attributes of rock glaciers is done, depending on the observation time windows of the moving areas (IPA Action Group RGIK - kinematic approach, 2020; RGIK - kinematic, 2022).

If the velocity class of a dominant moving area is characterized by an annual or multi-annual observation time window, a kinematic attribute “< cm/yr” or “cm/yr” is assigned with the respective velocity class of “< 1 cm/yr” and “1-3 cm/yr” (Table 2). The kinematic attribute “< cm/yr” is assigned even in the absence of detectable movement (i.e., without detected moving area(s)). If the velocity class of a dominant moving area is characterized by an observation time window shorter than one year (at least one month in the snow-free period), the kinematic attribute is assigned according to Table 2. These categories aim to obtain kinematic attributes as standardized as possible and reduce the operator’s subjectivity. The conversion from velocity classes to kinematic attributes considers the expected seasonal variations of rock glacier movement rate, generally higher

during summer periods, with minimum velocity occurring in early spring, velocity peaks in late spring and maximum velocity in late autumn (Berger et al., 2004; Cicoira et al., 2019; Delaloye and Staub, 2016; Wirz et al., 2016; Kenner et al., 2017; Cicoira et al., 2019; Wirz et al., 2016). The “undefined” category is chosen when (i) no (reliable) kinematic information is available (e.g., north/south-facing slopes, no data due to layover/shadow), (ii) the rock glacier is mainly characterized by a moving area of undefined velocity, or (iii) the heterogeneities of moving areas within rock glacier are too large.

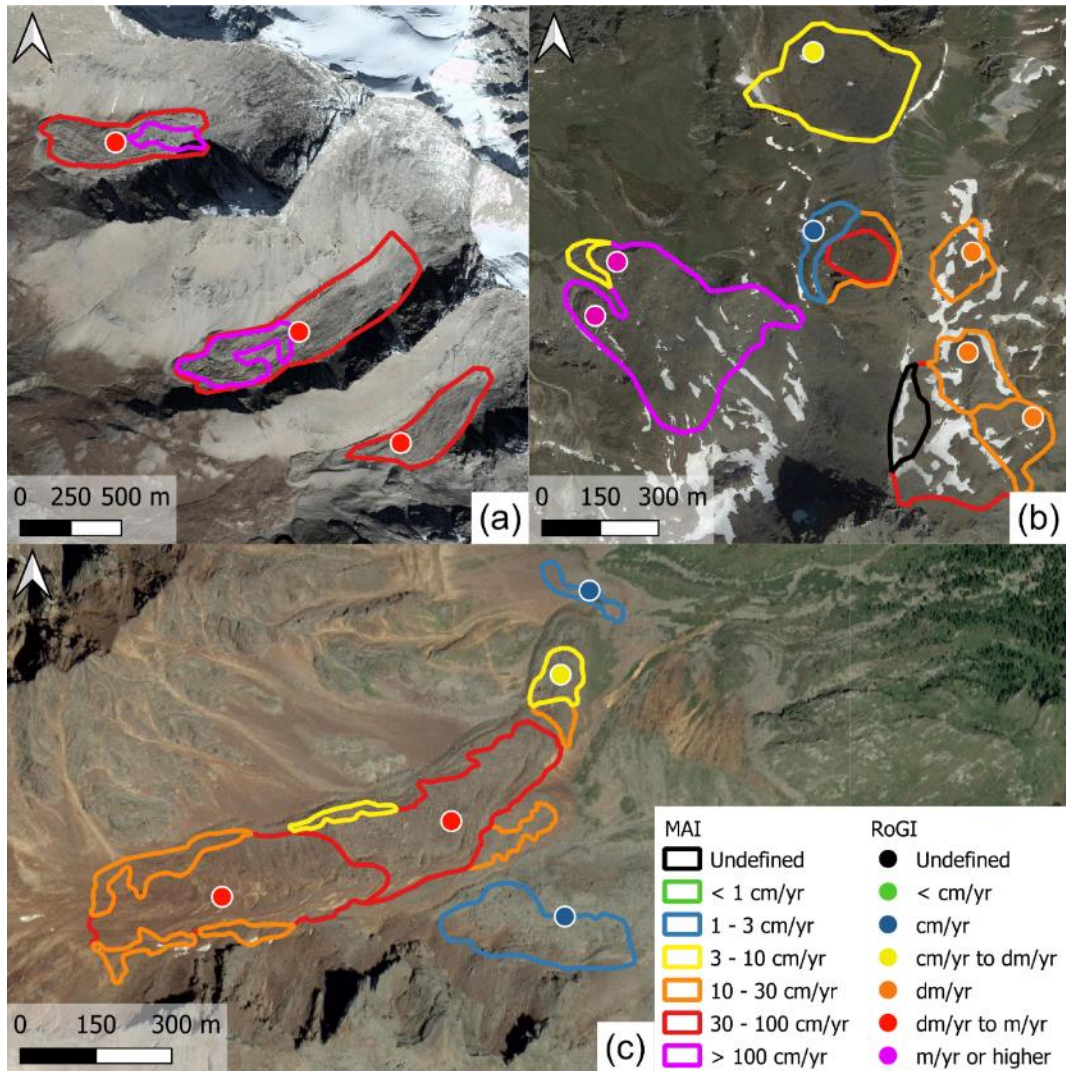
360 For each rock glacier, additional information is documented, such as the multi-year validity time frame (i.e., the years to which  
 the kinematic attributes apply) and the activity degree based on kinematic interpretation. According to the baseline concepts  
 (IPA Action Group RGIK - baseline concepts, 20220), “active” is assigned with coherent movement over most of the rock  
 glacier surface (displacement rate from decimeter to several meters per year), “transitional” with little to no movement over  
 most of the rock glacier surface (displacement rate less than decimeter per year in an annual mean), and “relict” without  
 365 detectable movement over most of its surface. This purely kinematic classification does not consider the permafrost content,  
 which is instead considered by other classifications proposed in the literature (e.g., Barsch, 1996). Information of the moving  
 area(s) used to assign kinematic attributes is also documented, such as the time characteristics (e.g., observation time window  
 and temporal frame) and the spatial representativeness, i.e., the qualitative estimation of the percentage of moving area(s)  
 370 surface inside the rock glacier unit compared to the total area of the rock glacier (e.g., < 50 %, 50-75 % and, > 75 %, also  
 qualitatively estimated if the rock glacier outline is not available from the existing inventory).

**Table 2. Description of the kinematic attribute categorization from the moving areas and the associated velocity classes, according to the IPA Action Group (IPA Action Group RGIK - baseline concepts, 20220; RGIK - kinematic, 2022).**

Observation time window	Associated velocity class <del>from to MA(s)</del>	Order of magnitude of RoG velocity	RoG kinematic attribute	Activity degree
≥ 1 year(s)	Undefined	-	Undefined	Undefined
≥ 1 year(s)	< 1 cm/yr	No/little movement	< cm/yr	Relict
< 1 year	1-3 cm/yr	≈ 0.01 m/yr	cm/yr	Transitional
< 1 year	3-10 cm/yr	≈ 0.05 m/yr	cm/yr to dm/yr	Transitional
< 1 year	10-30 cm/yr	≈ 0.1 m/yr	dm/yr	Active
< 1 year	30-100 cm/yr	≈ 0.5 m/yr	dm/yr to m/yr	Active
< 1 year	> 100 cm/yr	≈ 1 m/yr or more	m/yr or higher	Active
	-	Potential velocity	Other	-

## 4 Results

375 The moving areas and kinematic attributes compiled in the eleven investigated regions are shown in Fig. 4-6. A total of 5,077  
 moving areas covering about 5,140 km<sup>2</sup> are inventoried over 31,500 km<sup>2</sup> of investigated areas. The two different approaches  
 used to map and classify the moving areas (i.e., manual and semi-automated) show some differences. In Troms, Finnmark and  
 Nordenskiöld Land regions we observe a greater number of small, highly fragmented moving area outlines that fit InSAR pixel  
 boundaries without any smoothing (semi-automated approach, Fig. 5). In the other regions investigated with a manual  
 approach, outlines fit the detected slope movements with smooth outlines, and small moving areas (with slow velocities) are  
 380 frequently not mapped (Fig. 4 and 6).



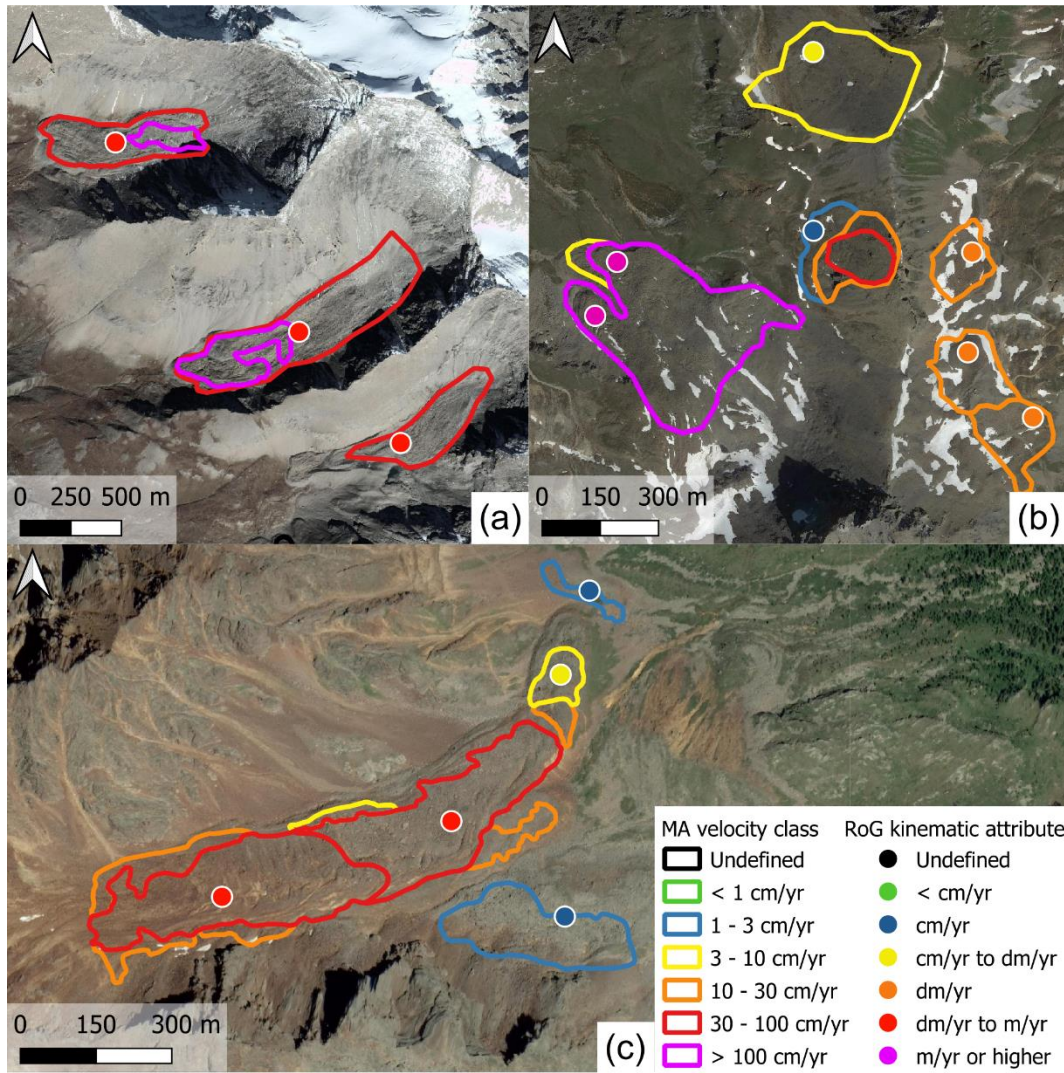
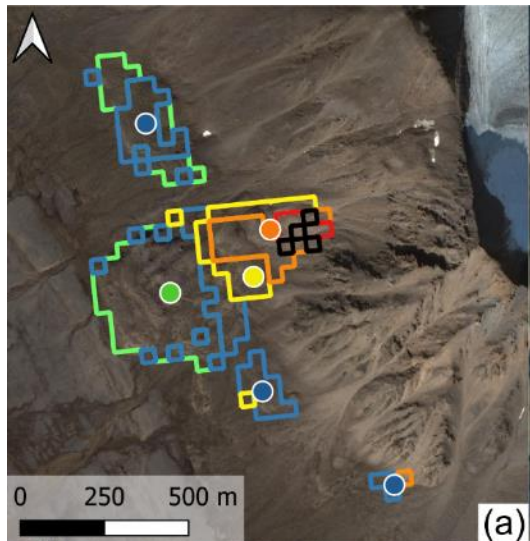
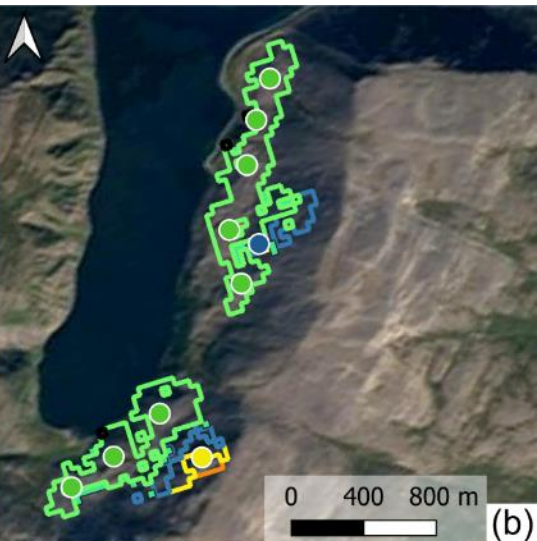


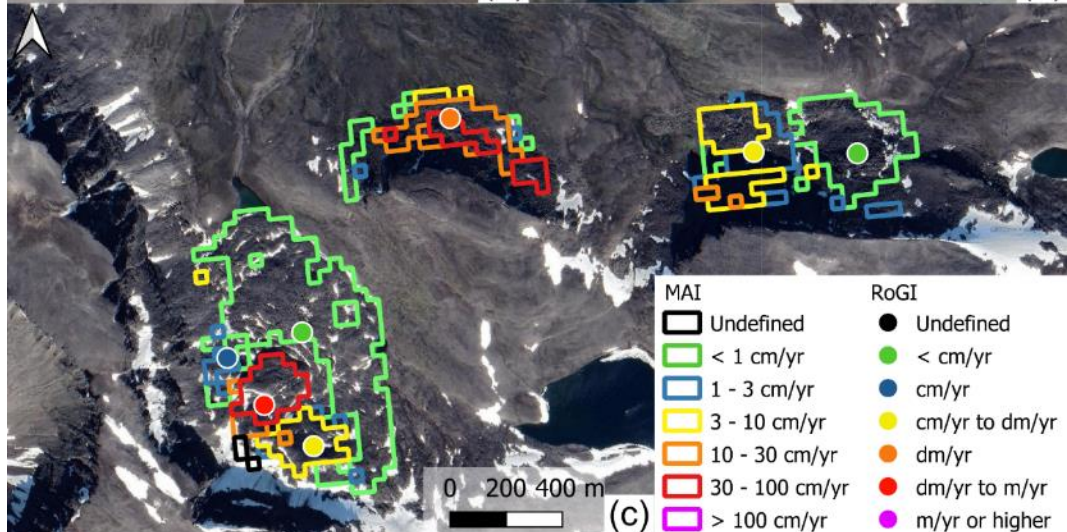
Figure 4. Examples of moving areas and rock glacier kinematic attributes produced for Vanoise (a, location: 45°16'10"N 7°03'00"E, 2900 m), Western Swiss Alps (b, location: 46°10'25"N 7°30'45"E, 2700 m), and Southern Venosta (c, location: 46°28'20"N 10°48'00"E, 2500 m). Orthoimages from © Google Earth 2019.



(a)



(b)



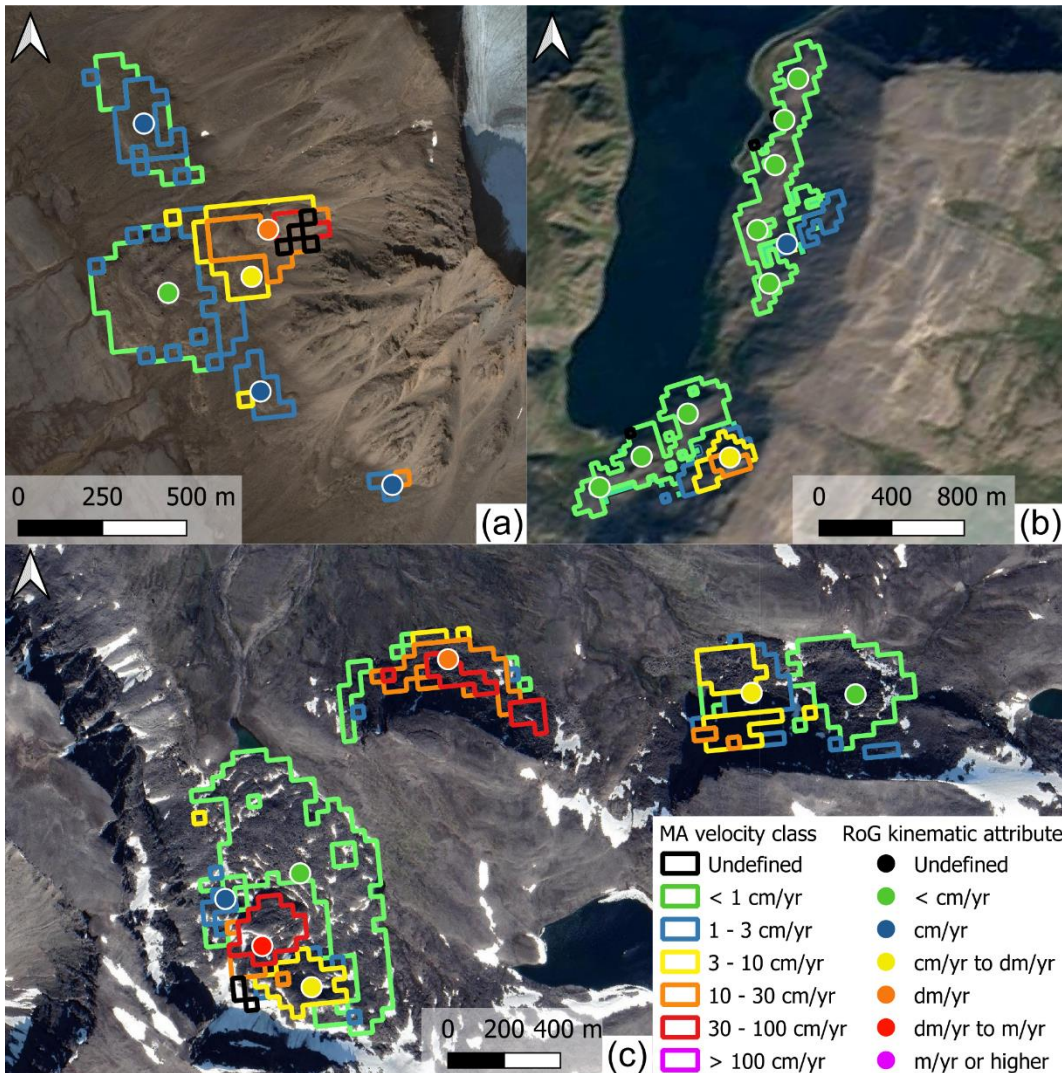
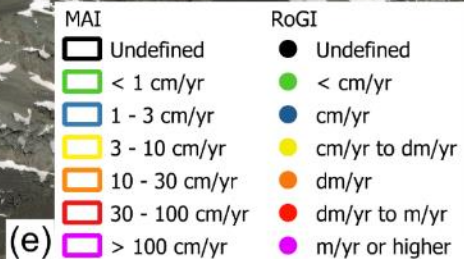
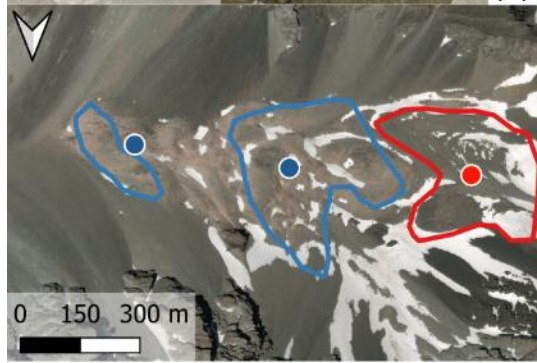
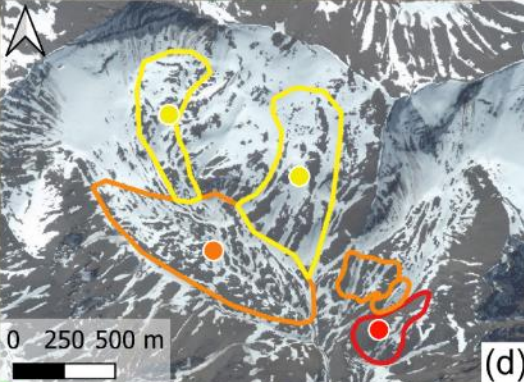
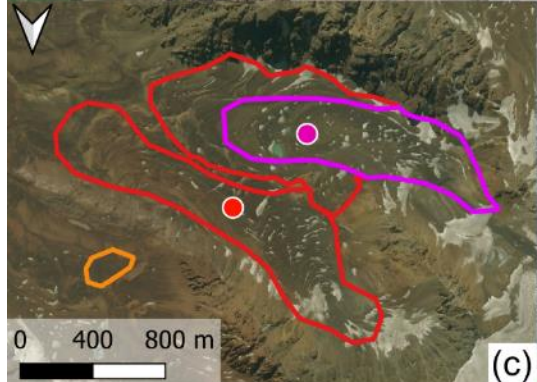
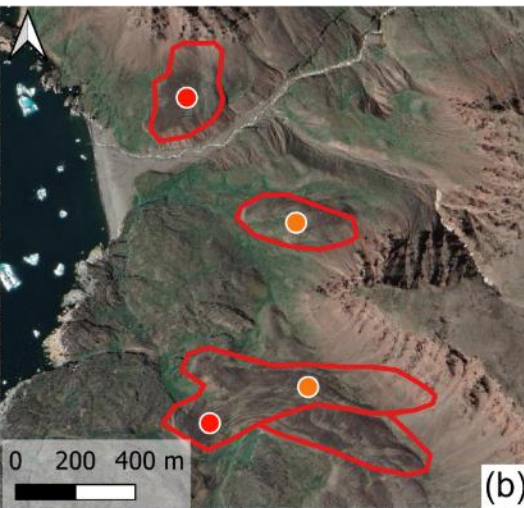
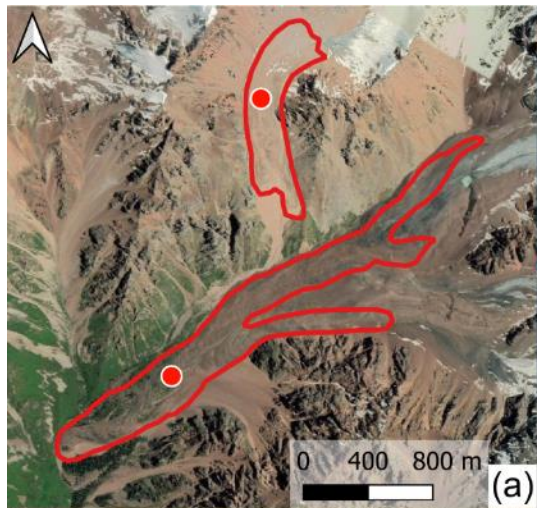


Figure 5. Examples of moving areas and rock glacier kinematic attributes produced for Nordenskiöld Land (a, location:  $77^{\circ}53'25''N$   $13^{\circ}55'35''E$ , 300 m), Finnmark (b, location:  $70^{\circ}44'50''N$   $28^{\circ}01'50''E$ , 100 m), and Troms (c, location:  $69^{\circ}26'45''N$   $20^{\circ}42'40''E$ , 920 m) based on a semi-automated multiple temporal baseline InSAR stacking procedure (Rouyet et al., 2021). Orthoimages from Norwegian Mapping Authority (<https://www.norgebilder.no/>; last access: 10 October 2021) © Google Earth 2019.



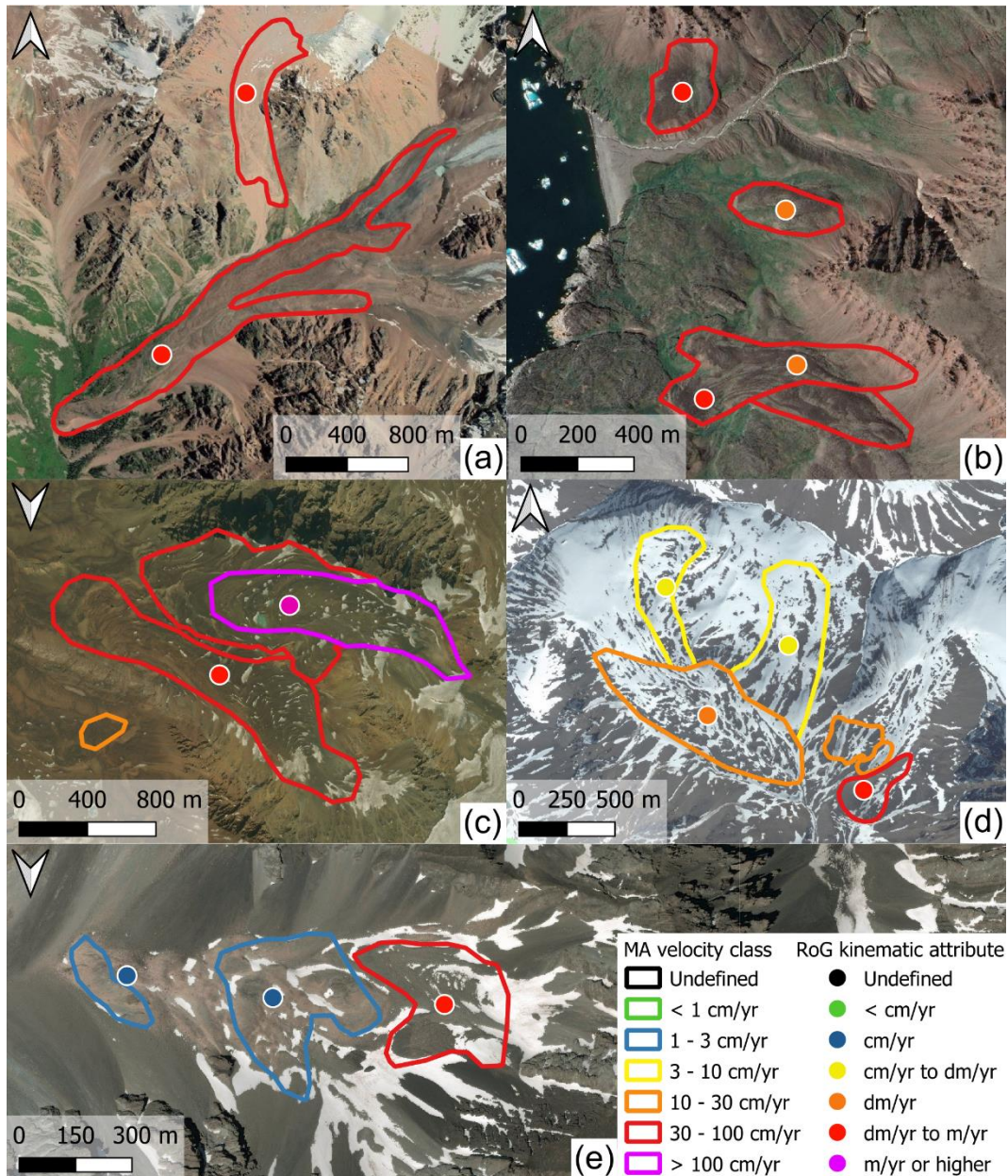


Figure 6. Examples of moving areas and rock glacier kinematic attributes produced for Northern Tien Shan (a, location: 43°06'00"N 77°12'20"E, 3400 m), Disko Island (b, location: 69°15'50"N 53°37'20"W, 100 m), Central Andes (c, location: 33°00'10"S 69°35'00"W, 4400 m), Brooks Range (d, location: 68°06'25"N 150°00'18"W, 1700 m) and Central Southern Alps (e, location: 43°35'40"S 170°44'00"E, 2000 m). Orthoimages from © Google Earth 2019.

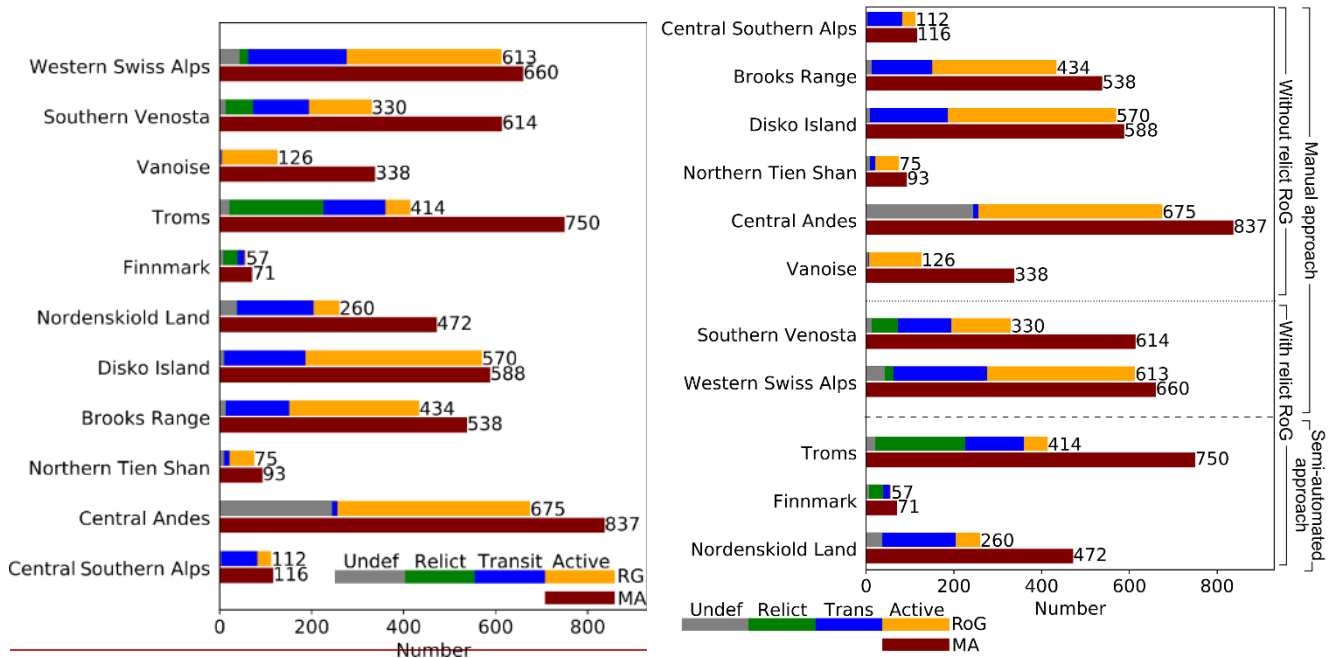
The number of mapped moving areas and their extent are quite different between the investigated regions. The number of mapped moving areas range from 71 (Finnmark) to 837 (Central Andes), sometime without a proportional increase in the total extent covered by moving areas (Fig. 7 [and](#), 8a [and](#) Table 3). Central Andes, Disko Island and Brooks Range are the regions

with a high number of moving areas and a high total extent covered by moving areas, while Troms, Western Swiss Alps and Southern Venosta have a high number of moving areas and a low total extent covered by moving areas (Fig. 8a). Accordingly, the first three regions have the largest moving areas visible from the boxplots of the area distributions (Fig. 8b), while the last three regions have smaller moving areas.

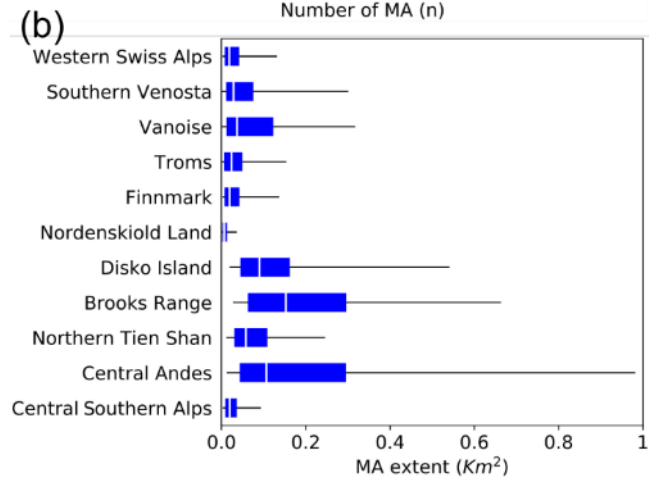
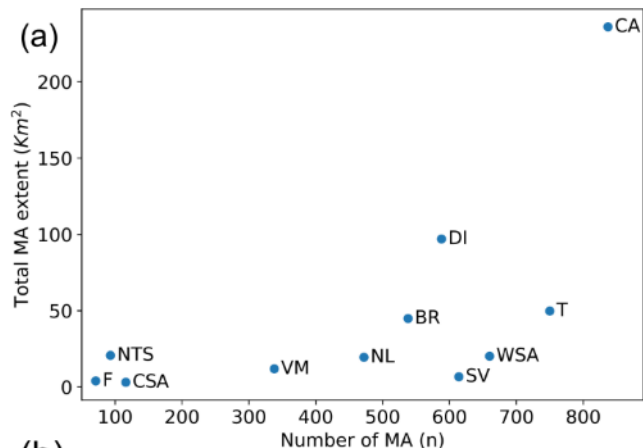
405 For Disko Island, Brooks Range, Vanoise, Central Andes, Northern Tien Shan, and the Western Swiss Alps region, most of the moving areas are classified with fast velocity classes (i.e., “30–100 cm/yr” and “> 100 cm/yr”; Fig. 9a and Table 3). In these regions, with the exception of Western Swiss Alps, few moving areas (less than 12 %) are classified with slow velocity classes (i.e., “< 1 cm/yr” and/or “1–3 cm/yr”). In the other regions, slow moving areas are prevalent, at the expense of faster ones. Therefore, in each region, the faster or slower moving areas seem to prevail over their counterparts.

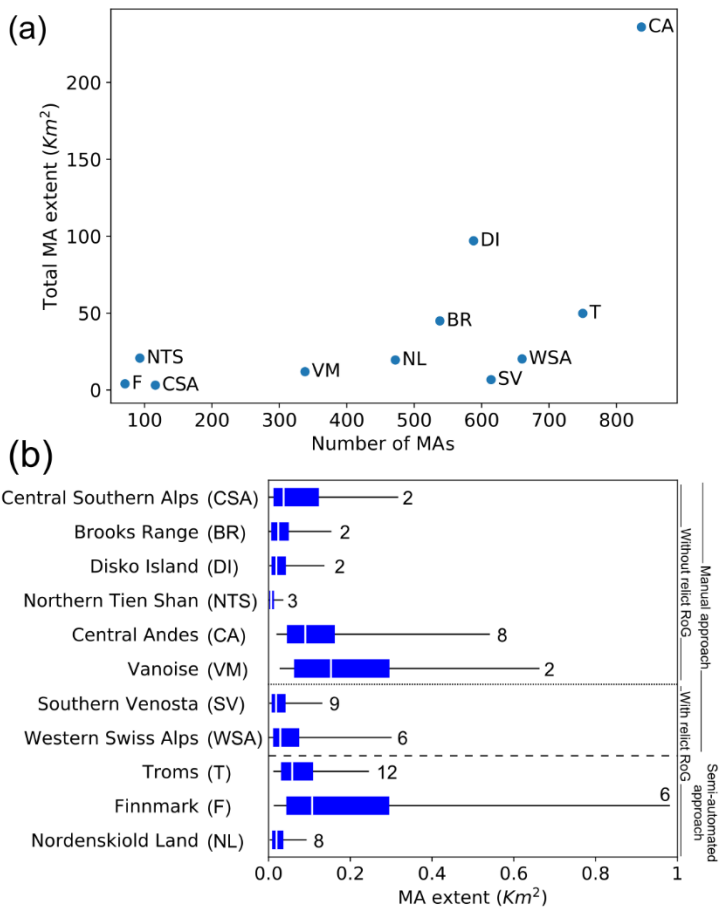
410 The number of classified rock glaciers is proportional with the number of detected moving areas, but there are fewer rock glaciers than moving areas are less numerous (Fig. 7). Therefore, this suggests each rock glacier often contains more than one moving area, as illustrated in Fig. 3. The maximum number of moving areas associated with a rock glacier goes ranges from a minimum of 2 up to 12 (Table 3 Fig. 8b). Southern Venosta, Troms, Nordenskiöld Land and Central Andes are the regions with the highest number of moving areas associated with one rock glacier, and also with a large number of moving areas mapped (Fig. 7 and 8a and Table 3).

415



420 Figure 7. Number of inventoried moving areas (brown bars), and rock glaciers classified as undefined (grey bars), relict (green bars), transitional (blue bars) and active (orange bars) for each investigated region. The size-length of the horizontal bars is proportional to the number of observations (x axis). The numbers to the right of the bars indicate the total number of moving areas and rock glaciers. Regional inventories are separated according to (i) the method used for mapping the MA (i.e., manual and semi-automated) and (ii) the inclusion/exclusion of relict rock glaciers that do not approach. Detailed information on assigned moving area velocity classes and rock glacier kinematic attributes are included in Table D1S3 and D2S4 of Supplementary material.

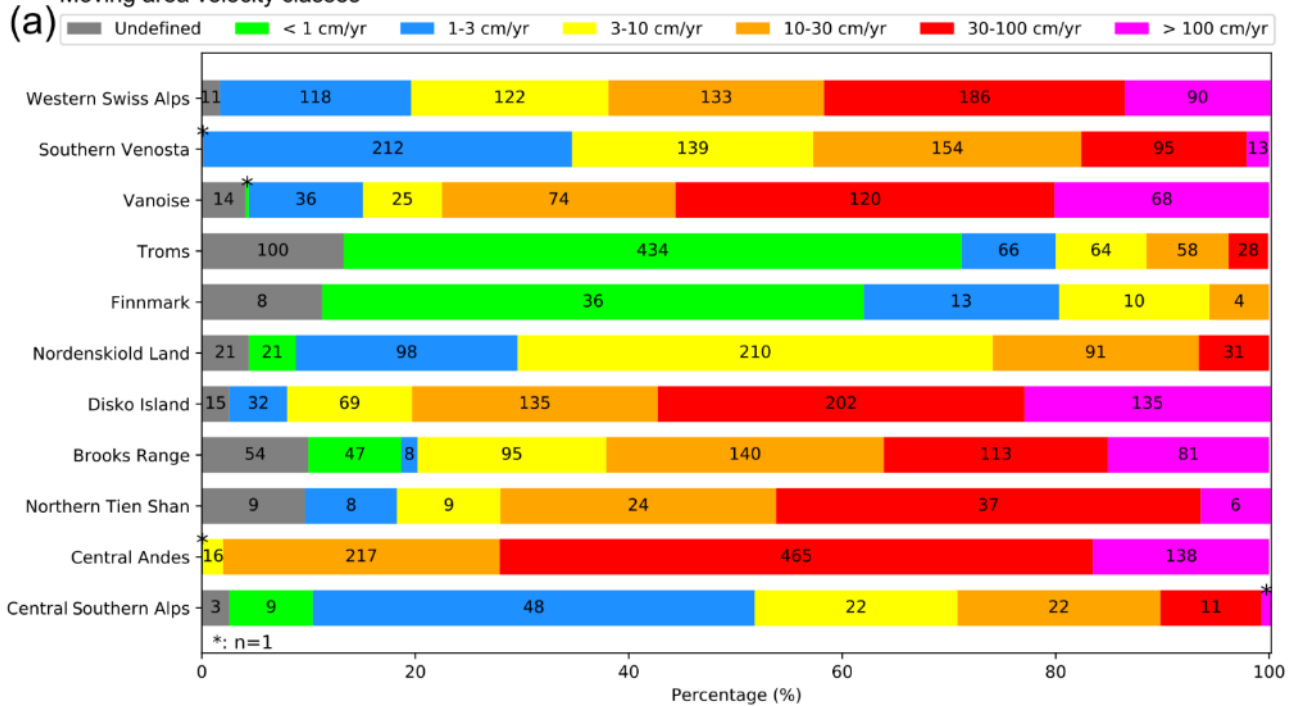




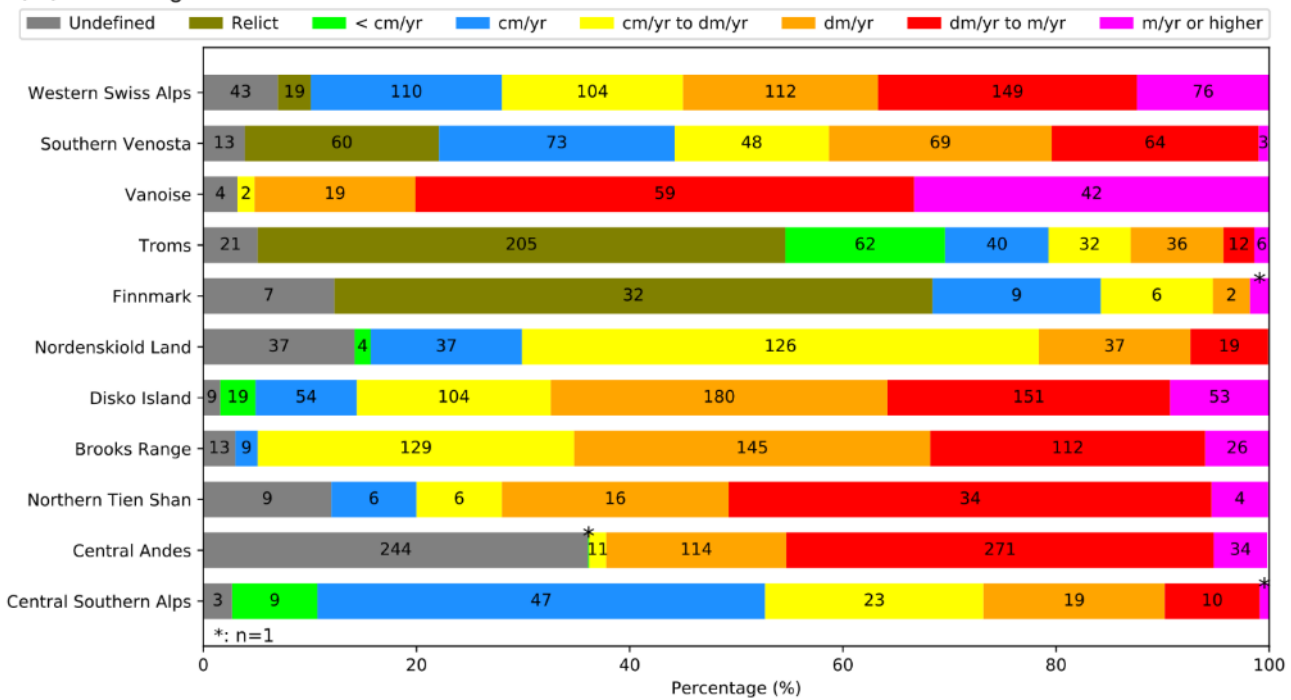
425 **Figure 8.** (a) Scatterplot of the total area covered by the moving areas (y axis) as a function of between the number of mapped moving areas (x axis) and the total area covered by the moving areas (y axis) for Nordenskiöld Land (NL), Disko Island (DI), Brooks Range (BR), Northern Tien Shan (NTS), Central Andes (CA), Central Southern Alps (CSA), Western Swiss Alps (WSA), Southern Venosta (SV), Vanoise Massif (VM), Troms (T) and Finnmark (F). (b) Boxplots show the area distribution of the moving areas. Bars enclose interquartile ranges, whiskers show 5 and 95 percentiles. On the right, the maximum number of MAs associated with one RoG for each region. Regional inventories that include relict rock glaciers (top) are separated from those that do not (centre) and from those investigated with a semi-automated approach (bottom). Regional inventories are separated according to (i) the method used for mapping the MA (i.e., manual and semi-automated) and (ii) the inclusion/exclusion of relict rock glaciers.

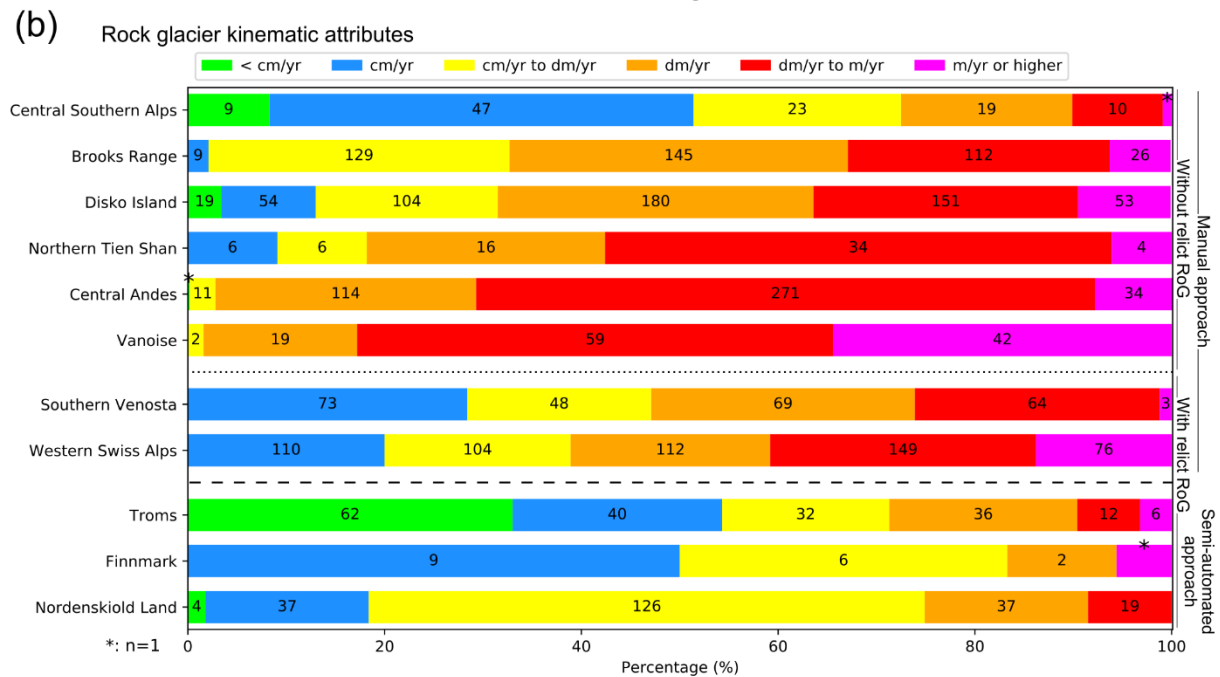
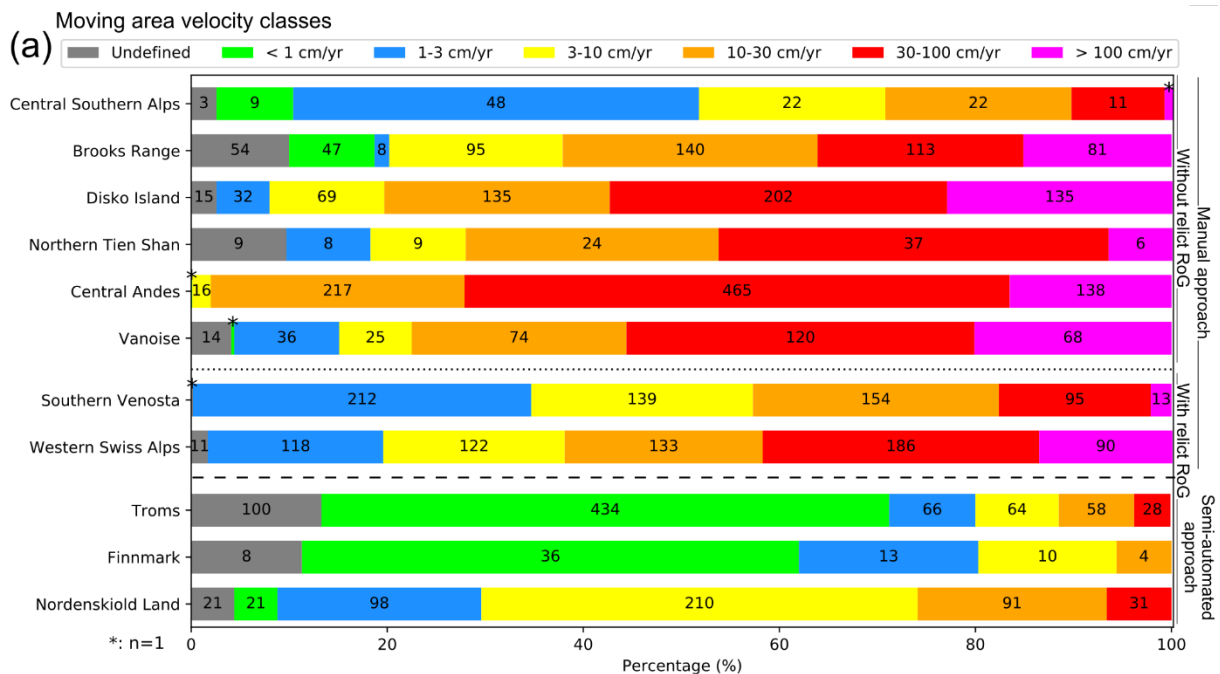
430

### Moving area velocity classes



### Rock glacier kinematic attributes





435

Figure 9. Assigned moving area velocity classes (a) and rock glacier kinematic attributes (b) for each investigated region. Relict landforms are not showed in panel b. The size\_length of the horizontal bars is proportional to the percentage (x axis), the values inside the bars are indicate the numbers for each category. Regional inventories that include relict rock glaciers (top) are separated from those that do not (centre) and from those investigated with a semi-automated approach (bottom). Regional inventories are separated according to (i) the method used for mapping the MA (i.e., manual and semi-automated) and (ii) the inclusion/exclusion

of relict rock glaciers. Detailed information on assigned moving area velocity classes and rock glacier kinematic attributes are included in Table D4S3 and D2S4 of Supplementary material.

**Table 3. Number of moving area velocity classes (percentage in brackets) and extent for each region.**

Region	Undefined (%)	↔ em/yr (%)	1–3 em/yr (%)	3–10 em/yr (%)	10–30 em/yr (%)	30– 100 em/yr (%)	>100 em/yr (%)	Total number MA	Total extension [km <sup>2</sup> ]	Total region extension [km <sup>2</sup> ]	Maximum number of MAs associated with one RG
Western Swiss Alps	11 (2)	0 (0)	118 (18)	122 (18)	133 (20)	186 (28)	90 (14)	660 (100)	20.2	1100	6
Southern Venosta	+	0 (1)	212 (34)	139 (23)	154 (25)	95 (15)	13 (2)	614 (100)	6.7	970	9
Vanoise	14 (4)	+	36 (11)	25 (7)	74 (22)	120 (35)	68 (20)	338 (100)	11.9	2000	2
Troms	100 (13)	434 (57)	66 (9)	64 (9)	58 (8)	28 (4)	0 (0)	750 (100)	49.8	4400	12
Finnmark	8 (11)	36 (51)	13 (18)	10 (14)	4 (6)	0 (0)	0 (0)	71 (100)	4	2600	6
Nordenskiöld Land	21 (4)	21 (4)	98 (21)	210 (45)	91 (19)	31 (7)	0 (0)	472 (100)	19.5	4100	8
Disko Island	15 (3)	0 (0)	32 (5)	69 (12)	135 (23)	202 (34)	135 (23)	588 (100)	97	7200	2
Brooks Range	54 (10)	47 (9)	8 (1)	95 (18)	140 (26)	113 (21)	81 (15)	538 (100)	44.9	1250	2
Northern Tien Shan	9 (10)	0 (0)	8 (9)	9 (10)	24 (26)	37 (39)	6 (6)	93 (100)	20.7	250	3
Central Andes	0 (1)	+	0 (1)	16 (2)	217 (26)	465 (55)	138 (46)	837 (100)	236	2900	8
Central Southern Alps	3 (3)	9 (8)	48 (41)	22 (19)	22 (19)	11 (9)	1 (1)	116 (100)	3.1	4800	2

Kinematic attributes are assigned at 3,666 rock glaciers investigated into the study regions. The number of classified rock 445 glaciers range between a maximum of 675 in Central Andes and a minimum of 57 in Finnmark (Fig. 7, Table 4). Rock glaciers with an “undefined” kinematic attribute are less than 15%, with the exception of Central Andes (36 %). Most of the rock glaciers are classified as active and transitional in all the regions investigated, with the exception of Troms (46 %) and Finnmark (32 %). Relict rock glaciers (i.e., without detected movements) are classified only in Troms (205; 49 %), Southern Venosta (60; 18 %), Finnmark (32; 56 %), and Western Swiss Alps (19; 3 %), while in the other regions they are not mapped in this work (Fig. 7) in the other regions for specific motivations explained below (Fig. 7, Table 4). In the Western Swiss Alps

region, the initial rock glacier inventory used to identify rock glaciers has been compiled following a “kinematic approach” (IPA Action Group RGIK - baseline concepts, 2022<sup>0</sup>), i.e., identifying and inventorying only rock glaciers with a detectable signal of movement, thus excluding relict landforms (Barboux et al., 2015). Consequently, when compiling the kinematic attributes in this region, a limited number of rock glaciers without detectable movements are classified. In the Nordenskiöld Land region, relict rock glaciers are not classified because the completely new inventory is also compiled with a “kinematic approach”. However, in the other regions, the initial inventories used to identify rock glaciers have been compiled with geomorphological approaches (IPA Action Group RGIK - baseline concepts, 2020<sup>2</sup>), i.e., recognizing and inventorying rock glaciers by a systematic visual inspection of geomorphological evidence on imaged landscape, DTM-derived products, as well as local field visits, thus including relict landforms (Ellis and Calkin, 1979; Humlum, 1982; Gorbunov, 1983; Mair et al., 2008; Humlum, 1982; Lilleøren and Etzelmüller, 2011; Sattler et al., 2016; Mair et al., 2008; Marcer et al., 2017; Sattler et al., 2016; Zalazar et al., 2020). In the Nordenskiöld Land region – characterised by continuous permafrost – there is no identified relict rock glacier. In the Vanoise, Brooks Range, Disko Island, Northern Tien Shan and Central Andes regions, kinematic analyses are conducted only on landforms identified by a clear InSAR signal of movement, thus without carrying out a thorough and comprehensive kinematic investigation of rock glaciers and excluding relict landforms. Also for this reason, slow-moving rock 465 glaciers (i.e., “< cm/yr” and/or “cm/yr”) are not mapped in Vanoise, and few slow-moving landforms are classified in the Brooks Range and Central Andes regions (Fig. 9b and Table 4). In Brooks Range and Disko Island regions, analyses on rock 470 glaciers without a clear signal of movement are also not conducted due to the lack of high-resolution optical imagery. In Central Southern Alps, a comprehensive kinematic investigation is conducted, but only rock glaciers with detectable movements are included in the inventory here presented.

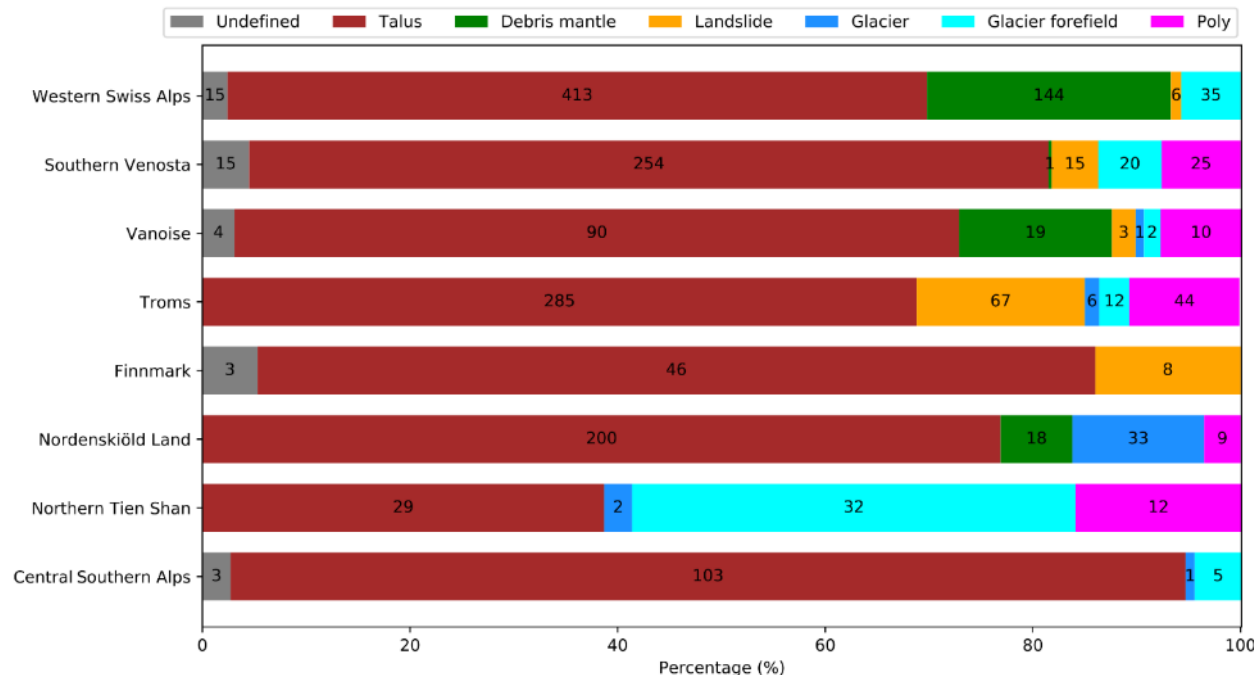
Looking in detail at the classifications, the kinematic attributes of rock glaciers reflect the velocity classes of moving areas, with most of rock glaciers in Disko Island, Brooks Range, Vanoise, Central Andes, Northern Tien Shan, and Western Swiss 475 Alps regions classified with fast kinematic attributes (i.e., “dm/yr to m/yr” and “m/yr or higher”), and a consistent portion of slow-moving rock glaciers (i.e., “< cm/yr” and/or “cm/yr”) in the other regions (Fig. 9b and Table 4). In Southern Venosta, Troms and Finnmark a large number of slow moving areas (i.e., “< 1 cm/yr” and/or “1-3 cm/yr”) are associated to slow-moving rock 480 glaciers.

**Table 4. Number of activity degrees and kinematic attributes assigned to rock glaciers (percentage in brackets) for each region.**

Region	Undefined (%)	Relict (%)	Transitional			Active			Total number	Total region RG (%)	Total region Extension [Km <sup>2</sup> ]
			<em/yr (%)	em/yr (%)	em/yr to dm/yr (%)	dm/yr (%)	dm/yr to m/yr (%)	m/yr or higher (%)			
Western Swiss Alps	43 (7)	19 (3)	0	110 (18)	104 (17)	112 (18)	149 (24)	76 (13)	613 (100)		1100
Southern Venosta	13 (4)	60 (18)	0	73 (22)	48 (15)	69 (21)	64 (19)	3 (1)	330 (100)		970
Vanoise	4 (3)	0	0	0	2 (2)	19 (15)	59 (47)	42 (33)	126 (100)		2000
Troms	21 (5)	205 (49)	62 (15)	40 (10)	32 (8)	36 (9)	12 (3)	6 (1)	414 (100)		4400
Finnmark	7 (12)	32 (56)	0	9 (16)	6 (11)	2 (3)	0	1 (2)	57 (100)		2600
Nordenskiöld Land	37 (14)	0	4 (2)	37 (14)	126 (49)	37 (14)	19 (7)	0	260 (100)		4100
Disko Island	9 (2)	0	19 (3)	54 (9)	104 (18)	180 (32)	151 (27)	53 (9)	570 (100)		7200
Brooks Range	13 (3)	0	0	9 (2)	129 (30)	145 (33)	112 (26)	26 (6)	434 (100)		1250
Northern Tien Shan	9 (12)	0	0	6 (8)	6 (8)	16 (21)	34 (46)	4 (5)	75 (100)		250
Central Andes	244 (36)	0	1 (1)	0	11 (2)	114 (16)	271 (40)	34 (5)	675 (100)		2900
Central Southern Alps	3 (3)	0	9 (8)	47 (42)	23 (20)	19 (17)	10 (9)	1 (1)	112 (100)		4800

Morphological characteristics of rock glaciers such as the upslope connections are examined and six main classes of upslope connection are assigned (Fig. 10) according to the IPA baseline concepts: talus, debris mantle, landslide, glacier, glacier forefield and poly connected (i.e., multiple connections) (IPA Action Group RGIK - baseline concepts, 2020). Unclear upslope connection ~~are-is~~ is classified as “Undefined.” This classification is not performed in Disko Island and Brooks Range, because the available optical data have too low resolution (greater than 10 m) to document this attribute. In the Central Andes region, the classification is not provided because of many cases with unclear upslope connection, ~~and~~ only glacier upslope connection ~~is separated and from~~ non-glacier upslope connection ~~are separated~~. For the Western Swiss Alps, Southern Venosta, Vanoise, Troms, Finnmark, Nordenskiöld Land, and Central Southern Alps regions, the highest number of rock glaciers is

classified with an upslope connection of talus type (at least 67 %). Only for the Tien Shan region is the glacier upslope connection type identified as the main class (43 %).



490 **Figure 10. Upslope connection classes for most of the investigated regions.** The size of the horizontal bars is proportional to the percentage (x axis), the values inside the bars are the numbers for each upslope connection class. Disko Island and Brooks Range regions are not shown because of lack of high-resolution optical data needed to document this attribute. The Central Andes region is not shown because of many cases with undefined upslope connection.

The validation of the assigned kinematic information is conducted on 30 rock glaciers with available DGNSS and feature tracking measurements acquired during the same time frame of InSAR measurements. The assigned moving area velocity classes sometimes do not fully cover the velocity ranges recorded by DGNSS measurements (Table 3). For 24 rock glaciers, the assigned moving area velocity classes and rock glacier kinematic attributes are in agreement with the available kinematic measurements. For four rock glaciers the assigned kinematics are-is slightly underestimated with InSAR, and for two rock glaciers the kinematics s are-is slightly overestimated (Table 35). Detailed results obtained from the validation are included in 500 Supplementary material B6 “Description of conducted validation”.

**Table 35: Validation conducted between the detected kinematic information (i.e., MA velocity classes and RoG kinematic attributes) and the independent datasets available for some regions.**

Region	Associated MA velocity classes [cm/yr]	RoG kinematic attribute	Validation dataset	Velocity recorded [m/yr]	Disagreement
Western Swiss Alps	> 100	m/yr or higher	DGNSS	0.7 – 2	
	> 100	m/yr or higher	DGNSS	0.7 – 2	
	30 – 100	dm/yr to m/yr	DGNSS	0.1 – 2.2	Underestimation
	1 – 3	cm/yr	DGNSS	0.025 – 0.035	
	> 100	m/yr or higher	DGNSS	0.75 – 0.8	Overestimation
	> 100	m/yr or higher	DGNSS	1.3	
	30 – 100	dm/yr to m/yr	DGNSS	1.9	Underestimation
	> 100	m/yr or higher	DGNSS	2.5 – 11	
	> 100	m/yr or higher	DGNSS	0.9 – 1.1	
	> 100	m/yr or higher	DGNSS	1.2 – 2.8	
Vanoise	3 – 10 and > 100	m/yr or higher	DGNSS	0.012 – 2.8	
	10 – 30 and > 100	m/yr or higher	DGNSS	0.5 – 2	
Troms	> 100	m/yr or higher	Feature tracking	1 – 2	
	30 – 100	dm/yr to m/yr	Feature tracking	0.5 – 1	
	30 – 100	dm/yr to m/yr	Feature tracking	0.5 – 1	
Nordenskiöld Land	1 – 3 and 3 – 10	cm/yr to dm/yr	DGNSS	0.024 – 0.05	
	< 1 and 1 – 3	< cm/yr	Feature tracking	0 – 0.02	
Brooks Range	> 100	m/yr or higher	DGNSS	13	
	> 100	m/yr or higher	DGNSS	2.1	
	> 100	m/yr or higher	DGNSS	5.7	
	> 100	m/yr or higher	DGNSS	0.9	Overestimation
Northern Tien Shan	> 100	m/yr or higher	Feature tracking	1 – 4	
	30 – 100	dm/yr to m/yr	Feature tracking	0.5 – 1	
	30 – 100	dm/yr to m/yr	Feature tracking	0.4 – 1	
	30 – 100	dm/yr to m/yr	Feature tracking	0.1 – 1.2	
	> 100	m/yr or higher	Feature tracking	2.3 – 2.8	
Central Andes	> 100	m/yr or higher	DGNSS	0.5 – 3.5	
	30 – 100	dm/yr to m/yr	DGNSS	> 1.5	Underestimation
Central Southern Alps	< 1	< cm/yr	DGNSS	0 – 0.03	Underestimation
	3 – 10	cm/yr to dm/yr	DGNSS	0.02 – 0.14	

### 5.1 Subjectivity of the method

The main problem for integrating standardized kinematic information within inventories compiled from different operators is the subjectivity of the operator himself in carrying out the work. The inherent degree of subjectivity is a typical source of uncertainty and variability within inventories compiled from remotely sensed imagery (Jones et al., 2018a; Brardinoni et al., 510 2019; Jones et al., 2018a). The proposed guidelines contain specific rules to guide the operator and reduce the operator's freedom to make specific choices, thus reducing and-limiting the subjectivity. Unlike other techniques, the InSAR signal provides an accurate measurement of movement, but the interpretation of the signal can still be affected by some degree of variability. T; therefore, the-multiple phases of correction and adjustment were conducted by a second operator were applied to further reduce the subjectivity and increase the overall reliability of the results. In addition, since the assigned moving area 515 velocity classes and rock glacier kinematic attributes refer to a range and not a precise value, which this contributes to further reduce the degree of subjectivity.

Despite the guidelines adopted, some degree of subjectivity can still occur. A large heterogeneity of the kinematics is often related to large spatial and temporal variability of the InSAR signal, — interpreted in different ways by the operators — or to errors. Therefore, before starting theis work on the eleven investigated sites, the operators involved in this work independently 520 tested the guidelines on two regions in the Western Swiss Alps. Such an inter-comparison exercise has shown to be a useful approach to evaluate the operator subjectivity (Brardinoni et al., 2019). Results of this inter-comparison exercise are included in a specific document of the ESA Permafrost\_CCI project (ESA - PVIR report, 2021). Outcomes show an increase in variability (i) in delineation and velocity classification of moving areas affected by large temporal- and spatial- variations in 525 velocityinterferograms, and (ii) in the kinematic classification of rock glaciers affected by a greater velocity heterogeneity of the related moving areas. However, often the same landforms have been classified with similar or adjacent classes, especially for fast landforms, because fast-moving classes include wider velocity ranges than slow-moving classes with smaller velocity ranges (ESA - PVIR report, 2021). Two examples are included in this paper (Fig. 11) to show the contrast between a simple rock glacier and a more complex one, characterized by higher variability of InSAR data. Results of theis inter-comparison 530 exercise were also useful in establishing more strict and clear rules to further reduce the subjectivity, and releasing the most refined version of the guidelines presented here. Furthermore, this initial stage conducted on two limited regions improved the knowledge and confidence of the method proposed by researchers.

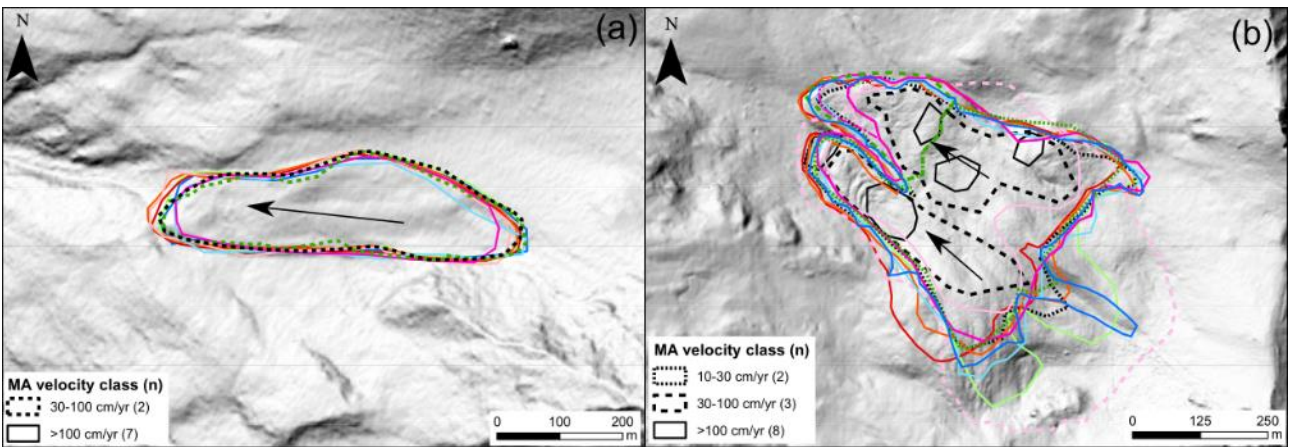


Figure 11. Two examples (a and b) of moving areas delineated by nine operators. Hillshade as background. The outlines drawn on the simple rock glacier (a) are very similar, and moving areas are classified as “>100 cm/yr” by seven operators and as “30-100 cm/yr” by two operators, due to because of the temporal variations in interferograms velocity. According to the mapped moving areas, this rock glacier is classified as “m/vr or higher” (also in agreement to GNSS data) by seven operators and as “dm/vr to m/vr” by two operators. Greater heterogeneity is observed on rock glacier affected by larger temporal- and spatial- variations in velocity interferograms (b), with more heterogeneous outlines of moving areas and different assigned velocity classes (“>100 cm/yr”, “30-100 cm/yr” and “10-30 cm/yr”). However, despite the larger heterogeneity, this rock glacier is classified as “m/vr or higher” by six operators and as “dm/vr to m/vr” by three operators; these kinematic attributes are in line with GNSS data, ranging from about 0.2 to 2 m/yr. Some related interferograms are included in Figures ES2-S4 of Supplementary material.

## 5.2 Dependencies related to moving area inventories

The guidelines presented here define rules that can be followed using different remote sensing techniques. In this work we used the InSAR technology, and therefore moving area inventories are affected by limitations related to radar interferometry

545 (Klees and Massonnet, 1998; Barboux et al., 2014; Klees and Massonnet, 1998; Strozzi et al., 2020). The use of the same sensors platforms (i.e., Sentinel-1 and ALOS-2) that share the same technical limits in all the investigated regions, however, simplifies the comparison evaluation between the moving area inventories.

The first limit related to InSAR is the general underestimation of displacements measured in the moving areas (Klees and Massonnet, 1998; Massonnet and Souyris, 2008). The downslope direction is generally assumed to represent the real 3D

550 movement of rock glaciers (Barboux et al., 2014), therefore the magnitude of displacement of moving areas on north- and south-facing slopes is more underestimated, even if both ascending and descending geometries are used.

The second limit related to InSAR concerns moving areas with slow movements (i.e., with velocities slower than 3 cm/yr), mainly investigated using annual interferograms with Sentinel-1 and ALOS-2 (Barboux et al., 2014; Yague-Martinez et al., 2016). With long time intervals (i.e., annual), the quality of the interferograms is lower due to loss of phase coherence (Klees and Massonnet, 1998; Touzi et al., 1999; Barboux et al., 2014; Bertone et al., 2019; Klees and Massonnet, 1998; Touzi et al., 1999).

Slow movements are therefore more complicated to be assessed with enough precision, and the reliability is consequently lower. For this reason, (i) the faster moving areas seem to prevail over their counterparts in some regions (Fig. 9a), and (ii) moving areas with velocity class “< 1 cm/yr” are probably not mapped in the Central Andes, Northern Tien Shan,

Disko Island, Vanoise, Southern Venosta, and the Swiss Alps regions (Fig. 9a and Table 3), where the focus is set on the more active landforms. In Troms and Finnmark regions, the large number of slow moving areas is related to the semi-automated method, able to better derive slow movements by exploiting a large set of interferograms with long time intervals.

Despite the limitations, InSAR is an appropriate tool for this exercise aimed at compiling kinematic inventories in as many representative periglacial regions worldwide as possible (Yague-Martinez et al., 2016). The InSAR image processing effort has been split across many sites. More advanced interferometric processing strategies such as Persistent Scatterer Interferometry (Ferretti et al., 2001; Crosetto et al., 2016; Ferretti et al., 2001) would allow to derive slow surface motion precisely, but the processing load is much more significant, and special attention has to be paid to the long-lasting snow-cover and the atmospheric stratification at high altitudes (Barboux et al., 2015; Osmanoglu et al., 2016).

To reduce the intrinsic limitations of InSAR, additional or alternative techniques may be used to support kinematic classification. For example, feature tracking (Monnier and Kinnard, 2017) and image cross correlation (Kääb, 2002; Necsoiu et al., 2016; Kääb et al., 2021; Necsoiu et al., 2016) conducted on ~~airborne~~ high resolution optical imagerys acquired from ~~airborne or spaceborne platforms~~ represent ~~a potential viable alternatives or complements to obtain technique to provide~~ kinematic information on large areas, ~~depending on the availability of optical images~~ (Kääb et al., 2021; Necsoiu et al., 2016). ~~Similarly, the differencing of sequential high resolution DTMs has been successfully used to quantify surface displacement and vertical change in particular (Kaab, 2008; Avian et al., 2009; Kaab, 2008). These techniques, although extremely useful for detecting large movements (i.e., topographic changes) with high accuracy over seasonal to annual and decadal time scales, rely heavily on the timing of costly repeat surveys, which typically have lower temporal resolution compared to SAR satellite-based acquisitions.~~

### 5.3 Characteristics related to the kinematic of rock glaciers

The guidelines used for assigning kinematic attributes to rock glaciers aim to be technology independent. However, (i) the kinematic information assigned refers only to periods documented ~~by~~ with InSAR data (snow-free seasons), and (ii) the inherent dynamic characteristics of the rock glacier can have impacts on the results. The seasonal variability (Berger et al., 2004; Ciccoira et al., 2019; Delaloye and Staub, 2016; Wirz et al., 2016; Kenner et al., 2017; Ciccoira et al., 2019; Wirz et al., 2016) is considered when the velocity classes of moving areas assigned during an observation time window of a few months are converted to kinematic attributes of rock glaciers (the latter refer to a multi-annual validity time frame, Table 2). However, the kinematic information might still be overestimated in cases where the rock glacier undergoes a strong seasonal acceleration. Furthermore, during to an observation time window of a few months (snow-free periods), local effects such as residual snow can further reduce the amount of available interferometric data. Coherent 6-days winter interferograms with Sentinel-1 could be used in the future to highlight the seasonal fluctuations (Strozzi et al., 2020).

The kinematic attributes assigned in this work provide general information about the kinematic status of rock glaciers only during the periods investigated with InSAR data, and without any monitoring purpose. Monitoring activities on rock glaciers are conducted using specific and more precise techniques (Delaloye et al., 2013; Fey and Krainer, 2020; Kääb et al., 2021;

Strozzi et al., 2020), and the approach here described can only support the identification of sites to start monitoring activities. However, kinematic information obtained from this approach can also be used as a support for future work on the calibration of permafrost numerical models (Böckli et al., 2012; Sattler et al., 2016; Westermann et al., 2017) and artificial intelligence algorithms (Böckli et al., 2012; Frauenfelder et al., 2008; Kofler et al., 2020; Robson et al., 2020).

In addition to the kinematic information, the high-quality optical data and the investigated connections of rock glaciers with other landforms (Fig. 10) provide useful information (Seppi et al., 2012; Necsoiu et al., 2016; Kääb et al., 2021; IPA Action Group RG IK - baseline concepts, 2020; Kääb et al., 2021; Necsoiu et al., 2016; Seppi et al., 2012); For example, in glacier-connected and glacier-forefield connected landforms, the distinction between rock glaciers and debris-covered glaciers is sometimes complicated (Berger et al., 2004; Bosson and Lambiel, 2016; Bolch et al., 2019; Bosson and Lambiel, 2016), and analyses of high-quality optical data help to discriminate the upper glacial part from the real lower rock glacier part. In the Central Andes region – where the upslope connections are often unclear – the distinctions between rock glaciers and debris-covered glaciers have not always been possible. Furthermore, the identification of glacier-connected and glacier-forefield connected rock glaciers is important to interpret improve the kinematic information, because these landforms are frequently characterized by ice melting that induce subsidence in summer time (Delaloye and Staub, 2016). The portion of rock glaciers potentially affected by consistent subsidence (i.e., glacier- and glacier-forefield upslope connected) is however lower than 13 % in the investigated regions, except in Northern Tien Shan region where it is around 45 %.

#### 5.4 Kinematic analysis of produced moving areas and rock glaciers

In the study region, a total of 5,077 moving areas were inventoried. in the investigated regions and These provide information on slope movements related surface deformation associated to rock glacier activity. Both manual and semi-automated methods are used in this work, but slight discrepancies are detected between these two approaches, with fragmented outlines that fit the pixel boundaries without any smoothing in Norway and Svalbard regions (Rouyet et al., 2021). Manually drawn moving areas better follow the standards defined in guidelines, smooth outlines fit the detected slope movements, and small moving areas (with slow velocities) are often not mapped. In our study, both application of manual and semi-automated methods are used and slight differences are observed has yielded some differences. We observe, with fragmented moving areas outlines that reflect fit the jagged edges of pixels (down to single-pixel moving areas) boundaries without any smoothing in Norway and Svalbard regions (Rouyet et al., 2021), whereas manually and smoothed outlines that fit the detected slope movements characterize the without small moving areas in the remaining other study regions. Clearly, Therefore, moving areas obtained infrom the semi-automated method (based on averaged unwrapped interferograms) are not directly comparable with those from the manual method counterparts (based on visual analyzes inspection of wrapped interferograms). However, the aim of this work is the integration of comparable kinematic information within rock glacier inventories; in this way, both methods allow to assign comparable kinematic attribute to rock glaciers, because the same rules are used to translate kinematic information from moving areas to rock glaciers, and the obtained moving areas share the same standards (e.g., velocity classes) established in the guidelines. Therefore, the choice between manual and rather than semi-automated methods should be made

625 according to the region extent and the available time, favoring semi-automated methods mainly for very large regions, where manual approaches take too much time.

Despite the slight ~~discrepancies~~differences detected in the moving area inventories, the kinematic attributes were successfully assigned to 3,666 rock glaciers, exploiting standardized rules to translate kinematic information from moving areas to rock glaciers. The main ~~discrepancies~~irregularities are related to the absence of rock glaciers classified as relict in the Vanoise, 630 ~~Nordenskiöld Land~~, Disko Island, Brooks Range, Northern Tien Shan, Central Andes, and Central Southern Alps regions (Fig. 7 ~~and Table 4~~). Only Southern Venosta, Troms and Finnmark regions include a consistent number of rock glaciers without detectable movements. In ~~Nordenskiöld Land and~~ Western Swiss Alps ~~regions~~, relict rock glaciers were not mapped because the method used to produce the rock glaciers ~~inventory~~ies exclude these landforms without movement. Therefore, the completeness of the inventories used to identify rock glaciers is essential to obtain a thorough and comprehensive kinematic 635 investigation. In Vanoise, Disko Island, Brooks Range, Northern Tien Shan, Central Andes, and Central Southern Alps regions relict rock glaciers were not mapped classified because the mapping~~classification~~ effort was placed only on faster moving landforms. The choice not to carry out analyses on rock glaciers without a clear signal of movement in these regions are due can be related to two reasons. First, the aim of this approach is to implement the kinematic information on~~of~~ rock glaciers in an active state~~affected by movement~~, without paying too much attention to the slowest landforms. Second, rock glaciers 640 without movements or with slow movements are more difficult to investigate, because the quality of the InSAR signal of yearly interferograms is generally lower, as explained above (Touzi et al., 1999; Barboux et al., 2014; Bertone et al., 2019; ~~Touzi et al., 1999~~); eConsequently, relict and slow-moving rock glaciers are more easily omitted or classified as undefined. For the above reasons, some compiled inventories only provide preliminary results, which still need improvement to be fully comprehensive~~and investigation~~. However, the use of InSAR data allowed to update the inventories, leading to a more accurate 645 classification, especially for active and transitional landforms.

The Preliminary results show a number of challenges that need to be addressed by the scientific community. For this reason, it is not possible to conduct detailed interpretations and comparisons between the investigated regions, which would require further investigations. However, we discuss an look at some preliminary considerations below. In this work we observed a large number of fast-moving rock glaciers (i.e., with kinematic attributes of “dm/yr to m/yr” and “m/yr or higher”) in the 650 Vanoise, Central Andes, and Northern Tien Shan regions (Fig. 9b ~~and Table 4~~). Higher velocity rates of rock glaciers in Northern Tien Shan and Central Andes than in the Alps have already been observed (Roer et al., 2005; Kääb et al., 2021; ~~Roer et al., 2005~~). However, as already documented by other authors (Roer et al., 2008; Delaloye et al., 2010, 2013; Delaloye and Staub, 2016; Marcer et al., 2019; ~~Roer et al., 2008~~; Seppi et al., 2019), there are also fast-moving rock glaciers situated on steep slopes in the Alps. In Troms, Finnmark and Nordenskiöld Land, the high number of slow-moving rock glaciers (i.e., “< cm/yr”, “cm/yr” and “cm/yr to dm/yr”) has also been observed in other studies (Eriksen et al., 2018; Kääb, 2002; Rouyet et al., 2019; Lilleøren et al., 2022). In contrast, little attention had been paid to the dynamics and evolution of rock glaciers in Brooks Range, Disko Island, and Central Southern Alps regions (Calkin, 1987; Sattler et al., 2016). tThis work therefore 655 presents preliminary~~first~~ results on the kinematics of rock glaciers in these study areas.

The quality of the assigned kinematic information was evaluated according to recent work (Strozzi et al., 2020; Kääb et al., 660 2021; Strozzi et al., 2020) on thirty landforms in all the investigated regions, except for Southern Venosta, Finnmark and Disko Island (Table 53). With reference to the main objective of this work, that is assigning a robust and reproducible kinematic attribute to rock glaciers, our classification resulted being correct in most cases. The four landforms underestimated may be related to the limits of the InSAR technique, such as the LOS orientation explained above, which generates underestimation especially on north- and south-facing slopes. On the other hand, the two landforms overestimated may be related to the high 665 seasonal variability of rock glaciers and the different observation time windows used to measure the movements between InSAR (i.e., summer ~~for fast moving landforms~~) and the validation dataset (i.e., annual). As explained above, the seasonal variability is considered when the velocity classes of moving areas are converted to kinematic attributes of rock glaciers. ~~However, if the rock glacier undergoes a strong seasonal acceleration, the assigned kinematic attributes might still be higher than the kinematic information available from the validation dataset.~~

## 670 5.5 Further application potential scenarios

This method holds potential for gaining new insight on rock glacier dynamics at a global scale. The spatial distribution of rock  
glaciers is frequently used as proxy for the past or present occurrence of permafrost (Haeberli, 1985; Boeckli et al., 2012;  
Schmid et al., 2015; Marcer et al., 2017), and the kinematics of these landforms can be used to derive indirect information  
about permafrost state. The methodology proposed in this work promotes the assignment of standardized kinematic attributes  
675 to rock glaciers, and therefore fosters the compilation of consistent information on permafrost at a global scale. Possible  
applications that will benefit from the proposed approach include the calibration of permafrost numerical models (Cremonese  
et al., 2011; Boeckli et al., 2012; Lilleøren et al., 2013; Schmid et al., 2015; Sattler et al., 2016; Marcer et al., 2017; Westermann  
et al., 2017) and artificial intelligence algorithms for assessing rock glacier activity over large areas (Frauenfelder et al., 2008;  
680 Boeckli et al., 2012; Kofler et al., 2020; Robson et al., 2020). Furthermore, indirect information on ice content within rock  
glaciers (Schmid et al., 2015; Marcer et al., 2017) may be used for water storage estimation (Bolch et al., 2009; Jones et al.,  
2018a). The methodology proposed in this work promotes standardized kinematic attributes assigned to rock glaciers, thus  
allowing to derive information on permafrost at a global scale, and support future work on the calibration of permafrost  
numerical models (Boeckli et al., 2012; Sattler et al., 2016; Westermann et al., 2017) and artificial intelligence algorithms  
applied to rock glaciers (Frauenfelder et al., 2008; Boeckli et al., 2012; Kofler et al., 2020; Robson et al., 2020). Furthermore,  
685 indirect information on ice content within rock glaciers (Schmid et al., 2015; Marcer et al., 2017) can also be used for applied  
purposes, such as water storage estimation (Bolch et al., 2009; Jones et al., 2018a) and permafrost distribution (Cremonese et  
al., 2011; Boeckli et al., 2012; Lilleøren et al., 2013; Schmid et al., 2015; Sattler et al., 2016; Marcer et al., 2017).  
The kinematic attributes assigned in this work are not intended for any monitoring purpose. The adopted standardized classes  
allow to reduce subjectivity at the expense of more precise velocities; in fact, the kinematics in most cases likely will not  
690 change so much in decades that a rock glacier shifts its kinematic class. Monitoring activities on rock glaciers are conducted  
using specific and more precise techniques (Delaloye et al., 2013; Fey and Krainer, 2020; Strozzi et al., 2020; Kääb et al..

2021), and the approach here described can only support the identification of sites to start monitoring activities. The kinematic attributes assigned in this work are not intended for any monitoring purpose. semi-quantitative categories In most cases, the kinematics of the rock glacier do not change much over the decades and a change in the of by more than one kinematic class is 695 not unlikely to occur. Monitoring activities on rock glaciers are conducted using specific and more precise techniques (Delaloye et al., 2013; Fey and Krainer, 2020; Strozzi et al., 2020; Kääb et al., 2021). In this context, the approach here described can only support (i) the identification of sites to start monitoring activities and (ii) the large-scale geohazard assessment in order to identify rock glaciers that may be a source of natural hazard (Delaloye et al., 2013; Kummert et al., 2018).

## 700 6 Conclusions

The method and the products presented here are the first results of an internationally coordinated work in which researchers from nine institutes applied common guidelines on eleven numerous regions worldwide, using spaceborne interferometric synthetic aperture radar interferometry measurements, to systematically integrate kinematic information within rock glacier inventories. Eleven Periglacial regions with different environmental settings parameters on both the Northern and Southern 705 Hemisphere are have been investigated. Despite the regional heterogeneity various regions and the intensive manual effort, the definition and application of common rules to include implement a rock glacier kinematic attribute within inventories have been feasible. It was possible to assign kinematic information to a majority of the investigated rock glacier inventories. However, in some regions, a greater larger number of landforms need to be validated, and rock glaciers with slow movements or without movements need to be investigated require further investigation. The achieved results The promising results derived 710 from the application of the InSAR-based standardized procedure open up new possibilities for the understanding rock glacier dynamics and the impact of climate change on sensitivity potential of permafrost degradation to climate change. Currently, these tasks are and numerical modelling of permafrost, mountain landscape dynamics, which until now had to be mainly based on in-situ detailed measurements of only a limited number of few landforms, if at all. In addition, the compiled inventories, even if still preliminary for some of them, will provide valuable opportune data for training, validation, and testing of artificial 715 intelligence and numerical modelling algorithms on rock glaciers using satellite imagery as well as numerical modelling of permafrost.

Further research – in both remote-sensing and fieldwork-based approaches – is needed to reduce the limitations associated with InSAR interferometry. Both the guidelines and the inventories still need improvement, e.g., the application of and more advanced InSAR processing strategies such as multi-temporal interferometric approaches, or different remote sensing 720 technologies such as feature tracking on optical airborne images could be applied. The lessons learned from the current study are critical in refining the proposed method and applying it widely to more regions.

## Supplementary material

The supplementary material includes the description of study areas (A), the tables of the attributes assigned to the moving areas (Table BS1) and rock glaciers (Table BS2), examples of moving areas classification (Figure S1), detailed tables of the moving area velocity classes (Table D1S3) and rock glacier kinematic attributes (Table S4D2), and the description of the conducted validation (BE) and examples of subjectivity observed (Figure S2FE, and FES3 and F3S4).

## Data Availability

The produced inventories are available at <https://www.unifr.ch/geo/geomorphology/en/research/cci-permafrost.html>, last access: 12 October 2021.

## 730 Author Contributions

CB, RD, LR and TS designed the study and managed the project. AB analysed data and wrote the manuscript. CB, RD, LR and TS contributed to analyse data and wrote the manuscript. AB, CB, XB, TB, FB, RC, HC, MD, RD, BE, OH, CL, KL, GP, LR, LRu produced the inventories. TS and LR produced the interferometric data. All authors contributed to the writing of the final version of the manuscript.

## 735 Financial support

This research was funded by the ESA Permafrost\_CCI project (grant number 4000123681/18/I-NB).

## Competing interests

The authors declare that the research was conducted in the absence of any commercial or financial relationships that could be

740 construed as a potential conflict of interest. Some authors are members of the editorial board of The Cryosphere. The peer-

review process was guided by an independent editor.

## Acknowledgments

The SAR data was processed with Gamma software. Moving area inventories and rock glaciers data were produced by the authors involved in this work. We thank the editor, the co-editor and the reviewers for their critical work which has allowed a considerable improvement of the manuscript.

Avian, M., Kellerer-Pirklbauer, A. and Bauer, A.: LiDAR for monitoring mass movements in permafrost environments at the cirque Hinteres Langtal, Austria, between 2000 and 2008, *Nat. Hazards Earth Syst. Sci.*, 9, 1087–1094, 2009.

Azócar, G. F. and Brenning, A.: Hydrological and geomorphological significance of rock glaciers in the dry Andes, Chile (27–33 S), *Permafr. Periglac. Process.*, 21(1), 42–53, 2010.

750 Barboux, C., Delaloye, R. and Lambiel, C.: Inventorying slope movements in an Alpine environment using DInSAR, *Earth Surf. Process. Landforms*, 39(15), 2087–2099, doi:10.1002/esp.3603, 2014.

Barboux, C., Strozzi, T., Delaloye, R., Wegmüller, U. and Collet, C.: Mapping slope movements in Alpine environments using TerraSAR-X interferometric methods, *ISPRS J. Photogramm. Remote Sens.*, 109, 178–192, doi:10.1016/j.isprsjprs.2015.09.010, 2015.

755 Barcaza, G., Nussbaumer, S. U., Tapia, G., Valdés, J., García, J.-L., Videla, Y., Albornoz, A. and Arias, V.: Glacier inventory and recent glacier variations in the Andes of Chile, South America, *Ann. Glaciol.*, 58(75pt2), 166–180, 2017.

Barsch, D.: Permafrost creep and rockglaciers, *Permafr. Periglac. Process.*, 3(3), 175–188, doi:10.1002/PPP.3430030303, 1992.

Barsch, D.: Rockglaciers: indicators for the Permafrost and Former Geoecology in High Mountain Environment, Springer Sci., 760 Berlin, Heidelberg, Germany, 1996.

Berger, J., Krainer, K. and Mostler, W.: Dynamics of an active rock glacier (Ötztal Alps, Austria), *Quat. Res.*, 62(03), 233–242, doi:10.1016/j.yqres.2004.07.002, 2004.

Berthling, I.: Beyond confusion: Rock glaciers as cryo-conditioned landforms, *Geomorphology*, 131(3–4), 98–106, doi:10.1016/J.GEOMORPH.2011.05.002, 2011.

765 Bertone, A., Zucca, F., Marin, C., Notarnicola, C., Cuozzo, G., Krainer, K., Mair, V., Riccardi, P., Callegari, M. and Seppi, R.: An Unsupervised Method to Detect Rock Glacier Activity by Using Sentinel-1 SAR Interferometric Coherence: A Regional-Scale Study in the Eastern European Alps, *Remote Sens.*, 11(14), 1711, doi:10.3390/rs11141711, 2019.

Blöthe, J. H., Rosenwinkel, S., Höser, T. and Korup, O.: Rock-glacier dams in High Asia, *Earth Surf. Process. Landforms*, 44(3), 808–824, doi:10.1002/esp.4532, 2019.

770 Blöthe, J. H., Halla, C., Schwalbe, E., Bottegal, E., Trombotto Liaudat, D. and Schrott, L.: Surface velocity fields of active rock glaciers and ice-debris complexes in the Central Andes of Argentina, *Earth Surf. Process. Landforms*, 46(2), 504–522, 2021.

Boeckli, L., Brenning, A., Gruber, S. and Noetzli, J.: A statistical approach to modelling permafrost distribution in the European Alps or similar mountain ranges, *Cryosph.*, 6, 125–140, doi:10.5194/tc-6-125-2012, 2012.

775 Bolch, T. and Gorbunov, A. P.: Characteristics and origin of rock glaciers in northern Tien Shan (Kazakhstan/Kyrgyzstan), *Permafr. Periglac. Process.*, 25(4), 320–332, 2014.

Bolch, T. and Strel, A.: Evolution of rock glaciers in northern Tien Shan, Central Asia, 1971 – 2016, in 5th European Conference on Permafrost, Chamonix, France, 23 June - 1 July 2018, pp. 48–49., 2018.

Bolch, T., Marchenko, S., Braun, L. N., Hagg, W., Severskiy, I. V and Young, G.: Significance of glaciers, rockglaciers and ice-rich permafrost in the Northern Tien Shan as water towers under climate change conditions, IHP/HWRP-Berichte, (8), 132–144, 2009.

Bolch, T., Rohrbach, N., Kutuzov, S., Robson, B. A. and Osmonov, A.: Occurrence, evolution and ice content of ice-debris complexes in the Ak-Shiirak, Central Tien Shan revealed by geophysical and remotely-sensed investigations, *Earth Surf. Process. Landforms*, 44(1), 129–143, 2019.

Bosson, J.-B. and Lambiel, C.: Internal Structure and Current Evolution of Very Small Debris-Covered Glacier Systems Located in Alpine Permafrost Environments, *Front. Earth Sci.*, 4, 39, doi:10.3389/feart.2016.00039, 2016.

Brardinoni, F., Scotti, R., Sailer, R. and Mair, V.: Evaluating sources of uncertainty and variability in rock glacier inventories, *Earth Surf. Process. Landforms*, 44(12), 2450–2466, doi:10.1002/esp.4674, 2019.

Brencher, G., Handwerger, A. L. and Munroe, J. S.: InSAR-based characterization of rock glacier movement in the Uinta Mountains, Utah, USA, *Cryosph.*, 15(10), 4823–4844, 2021.

Calkin, P. E.: Rock glaciers of central Brooks Range, Alaska, USA, *Rock glaciers*, 65–82, 1987.

Charbonneau, A. A. and Smith, D. J.: An inventory of rock glaciers in the central British Columbia Coast Mountains, Canada, from high resolution Google Earth imagery, *Arctic, Antarct. Alp. Res.*, 50(1), 1489026, doi:10.1080/15230430.2018.1489026, 2018.

Cicoira, A., Beutel, J., Faillettaz, J. and Vieli, A.: Water controls the seasonal rhythm of rock glacier flow, *Earth Planet. Sci. Lett.*, 528, 115844, doi:10.1016/J.EPSL.2019.115844, 2019.

Colucci, R. R., Boccali, C., Žebre, M. and Guglielmin, M.: Rock glaciers, protalus ramparts and pronival ramparts in the south-eastern Alps, *Geomorphology*, 269, 112–121, doi:10.1016/j.geomorph.2016.06.039, 2016.

Corte, A.: The hydrological significance of rock glaciers, *J. Glaciol.*, 17(75), 157–158, 1976.

Cremonese, E., Gruber, S., Phillips, M., Pogliotti, P., Boeckli, L., Noetzli, J., Suter, C., Bodin, X., Crepaz, A., Kellerer-Pirklbauer, A., Lang, K., Letey, S., Mair, V., Morra Di Cella, U., Ravanel, L., Scapozza, C., Seppi, R. and Zischg, A.: Brief communication: “An inventory of permafrost evidence for the European Alps,” *Cryosphere*, 5(3), 651–657, doi:10.5194/tc-5-651-2011, 2011.

Crosetto, M., Monserrat, O., Devanthéry, N., Cuevas-González, M., Barra, A. and Crippa, B.: Persistent scatterer interferometry using Sentinel-1 data, *Int. Arch. Photogramm. Remote Sens. Spat. Inf. Sci.*, 41(B7), 835–839, doi:10.5194/isprsarchives-XLI-B7-835-2016, 2016.

Darrow, M. M., Gyswytt, N. L., Simpson, J. M., Daanen, R. P. and Hubbard, T. D.: Frozen debris lobe morphology and movement: an overview of eight dynamic features, southern Brooks Range, Alaska, *Cryosph.*, 10(3), 977–993, 2016.

Delaloye, R. and Staub, B.: Seasonal variations of rock glacier creep: Time series observations from the Western Swiss Alps, in Proceedings of the International Conference on Book of Abstracts, Potsdam, Germany, 20-24 June 2016, pp. 20–24., 2016.

Delaloye, R., Lambiel, C. and Gärtner-Roer, I.: Overview of rock glacier kinematics research in the Swiss Alps, *Geogr. Helv.*, 65(2), 135–145, doi:10.5194/gh-65-135-2010, 2010.

Delaloye, R., Morard, S., Barboux, C., Abbet, D., Gruber, V., Riedo, M. and Gachet, S.: Rapidly moving rock glaciers in Matteringtal, *Jahrestagung der Schweizerischen Geomorphol. Gesellschaft*, 29, 21–31, 2013.

815 Delaloye, R., Barboux, C., Bodin, X., Brenning, A., Hartl, L., Hu, Y., Ikeda, A., Kaufmann, V., Kellerer-Pirklbauer, A. and Lambiel, C.: Rock glacier inventories and kinematics: A new IPA Action Group, in *Eucop5–5th European Conference of Permafrost*, Chamonix, France, 23 June - 1 July 2018, vol. 23, pp. 392–393., 2018.

Ellis, J. M. and Calkin, P. E.: Nature and distribution of glaciers, neoglacial moraines, and rock glaciers, east-central Brooks Range, Alaska, *Arct. Alp. Res.*, 11(4), 403–420, 1979.

820 Eriksen, H. Ø., Rouyet, L., Lauknes, T. R., Berthling, I., Isaksen, K., Hindberg, H., Larsen, Y. and Corner, G. D.: Recent acceleration of a rock glacier complex, Adjet, Norway, documented by 62 years of remote sensing observations, *Geophys. Res. Lett.*, 45(16), 8314–8323, 2018.

ESA - PVIR report: ESA CCI+ Permafrost. CCN1 & CCN2 Rock Glacier Kinematics as New Associated Parameter of ECV Permafrost. D4.1 Product Validation and Intercomparison Report (PVIR)., 825 [https://climate.esa.int/media/documents/CCI\\_PERMA\\_CCN1\\_2\\_D4.1\\_PVIR\\_v1.0\\_20210127.pdf](https://climate.esa.int/media/documents/CCI_PERMA_CCN1_2_D4.1_PVIR_v1.0_20210127.pdf), last access: 12 October 2021.

Falaschi, D., Tadono, T. and Masiokas, M.: Rock glaciers in the patagonian andes: an inventory for the monte san lorenzo (cerro cochrane) massif, 47° s, *Geogr. Ann. Ser. A, Phys. Geogr.*, 97(4), 769–777, doi:10.1111/geoa.12113, 2015.

Ferretti, A., Prati, C. and Rocca, F.: Permanent scatterers in SAR interferometry, *IEEE Trans. Geosci. Remote Sens.*, 39(1), 830 8–20, doi:10.1109/36.898661, 2001.

Fey, C. and Krainer, K.: Analyses of UAV and GNSS based flow velocity variations of the rock glacier Lazaun (Ötztal Alps, South Tyrol, Italy), *Geomorphology*, 365, 107261, doi:10.1016/j.geomorph.2020.107261, 2020.

Frauenfelder, R., Schneider, B. and Kääb, A.: Using dynamic modelling to simulate the distribution of rockglaciers, *Geomorphology*, 93(1–2), 130–143, doi:10.1016/J.GEOMORPH.2006.12.023, 2008.

835 Gorbunov, A. P., Seversky, E. V., Titkov, S. N., Marchenko, S. S. and Popov, M.: Rock glaciers, Zailiysiky Range, Kungei Ranges, Tienshan, Kazakhstan. National Snow and Ice Data Center/World Data Center for Glaciology, Boulder, CO, Digit. media, 1998.

Guglielmin, M. and Smiraglia, C.: The rock glacier inventory of the Italian Alps, 7th Int. Conf. Permafrost, Yellowknife, Canada. Univ. Laval Press. Nord., (55), 375–382, 1998.

840 Haeberli, W.: Creep of mountain permafrost: internal structure and flow of alpine rock glaciers, *Mitteilungen der Versuchsanstalt fur Wasserbau, Hydrol. und Glaziologie an der ETH Zurich*, 77, 1985.

Haeberli, W., Hallet, B., Arenson, L., Elconin, R., Humlum, O., Kääb, A., Kaufmann, V., Ladanyi, B., Matsuoka, N., Springman, S. and Mühl, D. V.: Permafrost creep and rock glacier dynamics, *Permafro. Periglac. Process.*, 17(3), 189–214, doi:10.1002/ppp.561, 2006.

845 Humlum, O.: Rock glacier types on Disko, central West Greenland, *Geogr. Tidsskr. J. Geogr.*, 82(1), 59–66, 1982.

~~IPA Action Group – baseline concepts: Towards standard guidelines for inventorying rock glaciers. Baseline concepts. Version 4.1., [https://bigweb.unifr.ch/Science/Geosciences/Geomorphology/Pub/Website/IPA/Guidelines/V4/200507\\_Baseline\\_Concepts\\_Inventorying\\_Rock\\_Glaciers\\_V4.1.pdf](https://bigweb.unifr.ch/Science/Geosciences/Geomorphology/Pub/Website/IPA/Guidelines/V4/200507_Baseline_Concepts_Inventorying_Rock_Glaciers_V4.1.pdf), last access: 8 October 2021, 2020.~~

850 ~~IPA Action Group – kinematic approach: Rock glacier inventory using InSAR (kinematic approach), Practical Guidelines v3.0.2., [https://bigweb.unifr.ch/Science/Geosciences/Geomorphology/Pub/Website/CCI/Guidelines/RGI\\_ka\\_InSAR-based\\_Guidelines\\_v.3.0.2.pdf](https://bigweb.unifr.ch/Science/Geosciences/Geomorphology/Pub/Website/CCI/Guidelines/RGI_ka_InSAR-based_Guidelines_v.3.0.2.pdf), last access: 8 October 2021, 2020.~~

Jones, D. B., Harrison, S., Anderson, K. and Betts, R. A.: Mountain rock glaciers contain globally significant water stores, *Sci. Rep.*, 8(1), 2834, doi:10.1038/s41598-018-21244-w, 2018a.

855 Jones, D. B., Harrison, S., Anderson, K., Selley, H. L., Wood, J. L. and Betts, R. A.: The distribution and hydrological significance of rock glaciers in the Nepalese Himalaya, *Glob. Planet. Change*, 160(August 2017), 123–142, doi:10.1016/j.gloplacha.2017.11.005, 2018b.

Kääb, A.: Monitoring high-mountain terrain deformation from repeated air- and spaceborne optical data: Examples using digital aerial imagery and ASTER data, *ISPRS J. Photogramm. Remote Sens.*, 57(1–2), 39–52, doi:10.1016/S0924-860 2716(02)00114-4, 2002.

Kääb, A., Chiarle, M., Raup, B. and Schneider, C.: Climate change impacts on mountain glaciers and permafrost, *Glob. Planet. Change*, 56(1–2), vii–ix, doi:10.1016/j.gloplacha.2006.07.008, 2007.

Kaab, A.: Remote sensing of permafrost-related problems and hazards, *Permafro. Periglac. Process.*, 136(1), 107–136, doi:10.1002/ppp, 2008.

865 Kääb, A., Strozzi, T., Bolch, T., Caduff, R., Trefall, H., Stoffel, M. and Kokarev, A.: Inventory and changes of rock glacier creep speeds in Ile Alatau and Kungöy Ala-Too, northern Tien Shan, since the 1950s, *Cryosph.*, 15(2), 927–949, 2021.

Kellerer-Pirklbauer, A., Delaloye, R., Lambiel, C., Gärtner-Roer, I., Kaufmann, V., Scapozza, C., Krainer, K., Staub, B., Thibert, E. and Bodin, X.: Interannual variability of rock glacier flow velocities in the European Alps, in 5th European Conference on Permafrost, June 2018, Chamonix, France, 23 June - 1 July 2018, pp. 396–397., 2018.

870 Kenner, R., Phillips, M., Beutel, J., Hiller, M., Limpach, P., Pointner, E. and Volken, M.: Factors Controlling Velocity Variations at Short-Term, Seasonal and Multiyear Time Scales, Ritigraben Rock Glacier, Western Swiss Alps, *Permafro. Periglac. Process.*, 684(May), 675–684, doi:10.1002/ppp.1953, 2017.

Klees, R. and Massonnet, D.: Deformation measurements using SAR interferometry: potential and limitations, *Geol. en Mijnb.*, 77(2), 161–176, doi:10.1023/A:1003594502801, 1998.

875 Kofler, C., Steger, S., Mair, V., Zebisch, M., Comiti, F. and Schneiderbauer, S.: An inventory-driven rock glacier status model (intact vs. relict) for South Tyrol, Eastern Italian Alps, *Geomorphology*, 350, 106887, 2020.

Konrad, S. K., Humphrey, N. F., Steig, E. J., Clark, D. H., Potter Jr, N. and Pfeffer, W. T.: Rock glacier dynamics and paleoclimatic implications, *Geology*, 27(12), 1131–1134, 1999.

880 [Krainer, K. and Ribis, M.: A Rock Glacier Inventory of the Tyrolean Alps \(Austria\), Austrian J. Earth Sci., 105, 32–47, 2012.](#)  
Kummert, M. and Delaloye, R.: Mapping and quantifying sediment transfer between the front of rapidly moving rock glaciers and torrential gullies, *Geomorphology*, 309, 60–76, 2018.

885 Kummert, M., Delaloye, R. and Braillard, L.: Erosion and sediment transfer processes at the front of rapidly moving rock glaciers: Systematic observations with automatic cameras in the western Swiss Alps, *Permafr. Periglac. Process.*, 29(1), 21–33, doi:10.1002/ppp.1960, 2018.

885 Lambiel, C., Strozzi, T., Paillex, N., Vivero, S. and Jones, N.: Mapping rock glaciers in the Southern Alps of New Zealand with Sentinel-1 InSAR, in 1st Southern Hemisphere Conference on Permafrost, Queenstown, New Zealand, 4-14 December 2019., 2019.

Lilleøren, K. S. and Etzelmüller, B.: A regional inventory of rock glaciers and ice-cored moraines in Norway, *Geogr. Ann. Ser. A, Phys. Geogr.*, 93(3), 175–191, 2011.

890 Lilleøren, K. S., Etzelmüller, B., Gärtner-Roer, I., Kääb, A., Westermann, S. and Guðmundsson, Á.: The distribution, thermal characteristics and dynamics of permafrost in Tröllaskagi, northern Iceland, as inferred from the distribution of rock glaciers and ice-cored moraines, *Permafr. Periglac. Process.*, 24(4), 322–335, 2013.

[Lilleøren, K. S., Etzelmüller, B., Rouyet, L., Eiken, T., and Hilbich, C.: Transitional rock glaciers at sea-level in Northern Norway, Earth Surf. Dynam. Discuss. \[preprint\], <https://doi.org/10.5194/esurf-2022-6>, in review, 2022.](#)

895 Liu, L., Millar, C. I., Westfall, R. D. and Zebker, H. A.: Surface motion of active rock glaciers in the Sierra Nevada, California, USA: inventory and a case study using InSAR, *Cryosph.*, 7(4), 1109–1119, doi:10.5194/tc-7-1109-2013, 2013.

Mair, V., Zischg, A., Stötter, J., Krainer, K., Zilger, J., Belitz, K., Schenk, A., Damm, B. and Bucher, K.: PROALP-Mapping and monitoring of permafrost phenomena in the Autonomous Province of Bolzano, Italy, in *Geophysical Research Abstracts*, p. 10., 2008.

900 Marcer, M.: Rock glaciers automatic mapping using optical imagery and convolutional neural networks, *Permafr. Periglac. Process.*, 31(4), 561–566, 2020.

Marcer, M., Bodin, X., Brenning, A., Schoeneich, P., Charvet, R. and Gottardi, F.: Permafrost Favorability Index: Spatial Modeling in the French Alps Using a Rock Glacier Inventory, *Front. Earth Sci.*, 5(December), doi:10.3389/feart.2017.00105, 2017.

905 Marcer, M., Serrano, C., Brenning, A., Bodin, X., Goetz, J. and Schoeneich, P.: Evaluating the destabilization susceptibility of active rock glaciers in the French Alps, *Cryosph.*, 13, 141–155, doi:10.5194/tc-13-141-2019, 2019.

Marcer, M., Ringsø Nielsen, S., Ribeyre, C., Kummert, M., Duvillard, P., Schoeneich, P., Bodin, X. and Genuite, K.: Investigating the slope failures at the Lou rock glacier front, French Alps, *Permafr. Periglac. Process.*, 31(1), 15–30, 2020.

910 Massonnet, D. and Feigl, K. L.: Radar interferometry and its application to changes in the Earth's surface, *Rev. Geophys.*, 36(4), 441–500, doi:10.1029/97RG03139, 1998.

Massonnet, D. and Souyris, J.-C.: Imaging with Synthetic Aperture Radar, EPFL Press, New York, 2008.

Matsuoka, M., Watanabe, T., Ikea, A., Christiansen, H. H., Humlum, O. and Rouyet, L.: Decadal-scale variability of polar rock glacier dynamics: accelerating due to warming?, in 1st Southern Hemisphere Conference on Permafrost, Queenstown, New Zealand, 4-14 December 2019., 2019.

915 [Monnier, S. and Kinnard, C.: Pluri-decadal \(1955-2014\) evolution of glacier-rock glacier transitional landforms in the central Andes of Chile \(30-33S\). Earth Surf. Dynam. 5, 493–509, doi:10.5194/esurf-5-493-2017, 2017](#)

Munroe, J. S.: Distribution, evidence for internal ice, and possible hydrologic significance of rock glaciers in the Uinta Mountains, Utah, USA, Quat. Res. (United States), 90(1), 50–65, doi:10.1017/qua.2018.24, 2018.

920 Necsoiu, M., Onaca, A., Wigginton, S. and Urdea, P.: Rock glacier dynamics in Southern Carpathian Mountains from high-resolution optical and multi-temporal SAR satellite imagery, Remote Sens. Environ., 177, 21–36, doi:10.1016/J.RSE.2016.02.025, 2016.

[Noetzli, J., Pellet, C. and Staub, B.: PERMOS reports, Cryospheric Comm. Swiss Acad. Sci., http://www.permos.ch/publications.html, last access: 14 October 2021, 2019.](#)

925 Osmanoğlu, B., Sunar, F., Wdowinski, S. and Cabral-Cano, E.: Time series analysis of InSAR data: Methods and trends, ISPRS J. Photogramm. Remote Sens., 115, 90–102, doi:10.1016/j.isprsjprs.2015.10.003, 2016.

[PERMOS: Permafrost in Switzerland 2014/2015 to 2017/2018. Noetzli, J., Pellet, C. and Staub, B. \(eds.\), Glaciological Report \(Permafrost\) No. 16-19 of the Cryospheric Commission of the Swiss Academy of Sciences, 104, doi:10.13093/permos-report-2019-16-19, http://www.permos.ch/publications.html, last access: 14 October 2021, 2019.](#)

930 Rangecroft, S., Harrison, S., Anderson, K., Magrath, J., Castel, A. P. and Pacheco, P.: A First Rock Glacier Inventory for the Bolivian Andes, Permafro. Periglac. Process., 25(4), 333–343, doi:10.1002/ppp.1816, 2014.

Reinosch, E., Gerke, M., Riedel, B., Schwalb, A., Ye, Q. and Buckel, J.: Rock glacier inventory of the western Nyainqāntanglha Range, Tibetan Plateau, supported by InSAR time series and automated classification, Permafro. Periglac. Process., in press, 2021.

[RGIK - baseline concepts: Towards standard guidelines for inventorying rock glaciers: baseline concepts \(Version 4.2.2\).](#)

935 [IPA Action Group Rock glacier inventories and kinematics, 13, https://bigweb.unifr.ch/Science/Geosciences/Geomorphology/Pub/Website/IPA/Guidelines/V4/220331\\_Baseline\\_Concepts\\_Inventorying\\_Rock\\_Glaciers\\_V4.2.2.pdf, last access: 16 May 2022.](#)

[RGIK - kinematic, 2022: Optional kinematic attribute in standardized rock glacier inventories \(Version 3.0\). IPA Action Group Rock glacier inventories and kinematics, 8.](#)

940 [https://bigweb.unifr.ch/Science/Geosciences/Geomorphology/Pub/Website/IPA/CurrentVersion/Current\\_KinematicalAttribute.pdf, last access: 16 May 2022.](#)

[RGIK - kinematic approach: Rock glacier inventory using InSAR \(kinematic approach\), Practical Guidelines \(Version 3.0.2\). IPA Action Group Rock glacier inventories and kinematics, 38, https://bigweb.unifr.ch/Science/Geosciences/Geomorphology/Pub/Website/CCI/Guidelines/RGI\\_ka\\_InSAR-based\\_Guidelines\\_v.3.0.2.pdf, last access: 8 October 2021, 2020.](#)

Robson, B. A., Bolch, T., MacDonell, S., Hölbling, D., Rastner, P. and Schaffer, N.: Automated detection of rock glaciers using deep learning and object-based image analysis, *Remote Sens. Environ.*, 250, 112033, doi:10.1016/j.rse.2020.112033, 2020.

950 Roer, I., Kääb, A. and Dikau, R.: Rockglacier acceleration in the Turtmann valley (Swiss Alps): Probable controls, *Nor. Geogr. Tidsskr.* - *Nor. J. Geogr.*, 59(2), 157–163, doi:10.1080/00291950510020655, 2005.

Roer, I., Haeberli, W., Avian, M., Kaufmann, V., Delaloye, R., Lambiel, C. and Kääb, A.: Observations and considerations on destabilizing active rock glaciers in the European Alps, Ninth Int. Conf. Permafrost, Univ. Alaska, Fairbanks, Alaska, June 29 - July 3, 2008, (4), 1505–1510, doi:10.5167/uzh-6082, 2008.

955 Rouyet, L., Lauknes, T. R., Christiansen, H. H., Strand, S. M. and Larsen, Y.: Seasonal dynamics of a permafrost landscape, Adventdalen, Svalbard, investigated by InSAR, *Remote Sens. Environ.*, 231, 111236, doi:10.1016/J.RSE.2019.111236, 2019.

Rouyet, L., Lilleøren, K., Böhme, M., Vick, L., Delaloye, R., Etzelmüller, B., Lauknes, T. R., Larsen, Y. and Blikra, L. H.: Regional InSAR inventory of slope movement in Northern Norway, Submitted to Frontiers in Earth Science, 2021. Regional morpho-kinematic inventory of slope movements in Northern Norway. Frontiers in Earth Science, 9:68188, doi10.3389/feart.2021.681088, 2021.

960 Sandwell, D. T. and Price, E. J.: Phase gradient approach to stacking interferograms, *J. Geophys. Res. Solid Earth*, 103(B12), 30183–30204, doi:<https://doi.org/10.1029/1998JB900008>, 1998.

Sattler, K., Anderson, B., Mackintosh, A., Norton, K. and de Róiste, M.: Estimating Permafrost Distribution in the Maritime Southern Alps, New Zealand, Based on Climatic Conditions at Rock Glacier Sites, *Front. Earth Sci.*, 4, 4, doi:10.3389/feart.2016.00004, 2016.

965 Schmid, M. O., Baral, P., Gruber, S., Shahi, S., Shrestha, T., Stumm, D. and Wester, P.: Assessment of permafrost distribution maps in the Hindu Kush Himalayan region using rock glaciers mapped in Google Earth, *Cryosphere*, 9(6), 2089–2099, doi:10.5194/tc-9-2089-2015, 2015.

Scotti, R., Brardinoni, F., Alberti, S., Frattini, P. and Crosta, G. B.: A regional inventory of rock glaciers and protalus ramparts in the central Italian Alps, *Geomorphology*, 186, 136–149, doi:10.1016/j.geomorph.2012.12.028, 2013.

970 Scotti, R., Crosta, G. B. and Villa, A.: Destabilisation of Creeping Permafrost: The Plator Rock Glacier Case Study (Central Italian Alps), *Permafro. Periglac. Process.*, 28(1), 224–236, doi:10.1002/ppp.1917, 2017.

Seppi, R., Carton, A., Zumiani, M., Dall'Amico, M., Zampedri, G. and Rigon, R.: Inventory, distribution and topographic features of rock glaciers in the southern region of the Eastern Italian Alps (Trentino), *Geogr. Fis. e Din. Quat.*, 35(2), 185–197, doi:10.4461/GFDQ.2012.35.17, 2012.

975 Seppi, R., Carturan, L., Carton, A., Zanoner, T., Zumiani, M., Cazorzi, F., Bertone, A., Baroni, C. and Salvatore, M. C.: Decoupled kinematics of two neighbouring permafrost creeping landforms in the Eastern Italian Alps, *Earth Surf. Process. Landforms*, 44(13), 2703–2719, doi:10.1002/esp.4698, 2019.

Strozzi, T., Caduff, R., Jones, N., Barboux, C., Delaloye, R., Bodin, X., Kääb, A., Mätzler, E. and Schrott, L.: Monitoring rock glacier kinematics with satellite synthetic aperture radar, *Remote Sens.*, 12(3), 559, doi:10.3390/rs12030559, 2020.

980 Touzi, R., Lopes, A., Bruniquel, J. and Vachon, P. W.: Coherence estimation for SAR imagery, *IEEE Trans. Geosci. Remote Sens.*, 37(1), 135–149, doi:10.1109/36.739146, 1999.

Villarroel, C., Tamburini Beliveau, G., Forte, A., Monserrat, O., Morvillo, M., Villarroel, C. D., Tamburini Beliveau, G., Forte, A. P., Monserrat, O. and Morvillo, M.: DInSAR for a Regional Inventory of Active Rock Glaciers in the Dry Andes Mountains of Argentina and Chile with Sentinel-1 Data, *Remote Sens.*, 10(10), 1588, doi:10.3390/rs10101588, 2018.

985 Wagner, T., Pleschberger, R., Kainz, S., Ribis, M., Kellerer-Pirklbauer, A., Krainer, K., Philippitsch, R. and Winkler, G.: The first consistent inventory of rock glaciers and their hydrological catchments of the Austrian Alps, *Austrian J. Earth Sci.*, 113(1), 1–23, 2020.

Wang, X., Liu, L., Zhao, L., Wu, T., Li, Z. and Liu, G.: Mapping and inventorying active rock glaciers in the northern Tien Shan of China using satellite SAR interferometry, *Cryosphere*, 11(2), 997–1014, doi:10.5194/tc-11-997-2017, 2017.

990 Westermann, S., Peter, M., Langer, M., Schwamborn, G., Schirrmüller, L., Etzelmüller, B. and Boike, J.: Transient modeling of the ground thermal conditions using satellite data in the Lena River delta, Siberia, *Cryosph.*, 11, 1441–1463, doi:10.5194/tc-11-1441-2017, 2017.

Wirz, V., Gruber, S., Purves, R. S., Beutel, J., Gärtner-Roer, I., Gubler, S. and Vieli, A.: Short-term velocity variations at three rock glaciers and their relationship with meteorological conditions, *Earth Surf. Dyn.*, 4(1), 103–123, doi:10.5194/esurf-4-103-995 2016, 2016.

Yague-Martinez, N., Prats-Iraola, P., Rodriguez Gonzalez, F., Brcic, R., Shau, R., Geudtner, D., Eineder, M. and Bamler, R.: Interferometric Processing of Sentinel-1 TOPS Data, *IEEE Trans. Geosci. Remote Sens.*, 54(4), 2220–2234, doi:10.1109/TGRS.2015.2497902, 2016.

Yu, C., Li, Z. and Penna, N. T.: Interferometric synthetic aperture radar atmospheric correction using a GPS-based iterative 1000 tropospheric decomposition model, *Remote Sens. Environ.*, 204, 109–121, doi:10.1016/J.RSE.2017.10.038, 2018.

Zalazar, L., Ferri, L., Castro, M., Gargantini, H., Gimenez, M., Pitte, P., Ruiz, L., Masiokas, M., Costa, G. and Villalba, R.: Spatial distribution and characteristics of Andean ice masses in Argentina: results from the first National Glacier Inventory, *J. Glaciol.*, 66(260), 938–949, 2020.

Zwieback, S., Liu, X., Antonova, S., Heim, B., Bartsch, A., Boike, J. and Hajnsek, I.: A statistical test of phase closure to 1005 detect influences on DInSAR deformation estimates besides displacements and decorrelation noise: Two case studies in high-latitude regions, *IEEE Trans. Geosci. Remote Sens.*, 54(9), 5588–5601, 2016.